

University of Montreal

**Role of the *Protein Tyrosine Kinase 7* gene in human neural
tube defects**

By Mingqin Wang

Program of Biomedical Sciences
Faculty of Medicine

Thesis presented to Faculty of Medicine
in order to obtain the degree of Masters
In Biomedical Sciences

June 2015

© Mingqin Wang, 2015

Abstract

Neural tube defects (NTDs) are among the most common congenital defects with a high incidence of 1-2 per 1000 births, causing a heavy burden to both the families and society. Various types of NTDs result from defects happening in the neurulation process during vertebrate embryonic development. In order to prevent the occurrence of NTDs, understanding the underlying mechanism is a prerequisite. The etiology of NTDs is complex involving environmental and genetic factors. Folic acid supplementation was proven to efficiently decrease the frequency of NTDs by 50-70% depending on the time point of this supplementation and demographic background. Gene identification studies in NTDs have adopted mainly a candidate gene approach investigating folate-related genes and genes derived from animal models. In particular, studies in mouse models have demonstrated a strong association between the non canonical Wnt/Planar Cell Polarity (PCP) pathway and NTDs. *Protein Tyrosine Kinase 7 (PTK7)* is a member of the PCP pathway and was shown to cause a very severe form of NTDs called craniorachischisis in a mouse model. *Ptk7* genetically interacts with a core PCP member *Vangl2* where double heterozygotes suffer from spina bifida. These data make *PTK7* a strong candidate for NTDs in humans. We sequenced the coding region and the exon-intron junctions of *PTK7* in a cohort of 473 patients affected with various forms of open and closed NTDs. Novel and rare variants (<1%) were genotyped in a cohort of 473 individuals. Their pathogenic effect was predicted *in silico* and functionally in an overexpression assay in a well established zebrafish model. We identified in our cohort 6 novel rare mutations, 3 of which are absent in all public databases, in 1.1% of our NTD cohort. One variant, p.Gly348Ser, acted as a hypermorph when overexpressed in the zebrafish model. Our findings implicate mutation of *PTK7* as a risk factor for NTDs and provide additional evidence for a pathogenic role of PCP signaling in these malformations.

Keywords: Protein Tyrosine Kinase 7, neural tube defects, planar cell polarity, convergent extension, re-sequencing analysis, zebrafish model.

Résumé

Les anomalies du tube neural (ATN) sont des anomalies développementales où le tube neural reste ouvert (1-2/1000 naissances). Afin de prévenir cette maladie, une connaissance accrue des processus moléculaires est nécessaire. L'étiologie des ATN est complexe et implique des facteurs génétiques et environnementaux. La supplémentation en acide folique est reconnue pour diminuer les risques de développer une ATN de 50-70% et cette diminution varie en fonction du début de la supplémentation et de l'origine démographique. Les gènes impliqués dans les ATN sont largement inconnus. Les études génétiques sur les ATN chez l'humain se sont concentrées sur les gènes de la voie métabolique des folates du à leur rôle protecteur dans les ATN et les gènes candidats inférés des souris modèles. Ces derniers ont montré une forte association entre la voie non-canonique Wnt/polarité cellulaire planaire (PCP) et les ATN. Le gène *Protein Tyrosine Kinase 7* est un membre de cette voie qui cause l'ATN sévère de la craniorachischisis chez les souris mutantes. *Ptk7* interagit génétiquement avec *Vangl2* (un autre gène de la voie PCP), où les doubles hétérozygotes montrent une spina bifida. Ces données font de *PTK7* comme un excellent candidat pour les ATN chez l'humain. Nous avons re-séquencé la région codante et les jonctions intron-exon de ce gène dans une cohorte de 473 patients atteints de plusieurs types d'ATN. Nous avons identifié 6 mutations rares (fréquence allélique <1%) faux-sens présentes chez 1.1% de notre cohorte, dont 3 sont absentes dans les bases de données publiques. Une variante, p.Gly348Ser, a agi comme un allèle hypermorphique lorsqu'elle est surexprimée dans le modèle de poisson zèbre. Nos résultats impliquent la mutation de *PTK7* comme un facteur de risque pour les ATN et supporte l'idée d'un rôle pathogène de la signalisation PCP dans ces malformations.

Mots clefs: Protéine Tyrosine Kinase 7, anomalies du tube neural, polarité cellulaire planaire, extension convergence, analyses de re-séquençage, modèle poisson zèbre

Table of contents

1 Introduction.....	1
1.1 Neural tube defects.....	1
1.1.1 Classification and clinical symptoms.....	1
1.1.2 The epidemiology	3
1.1.3 Aetiology of NTDs.....	3
1.1.3.1 Folic acid	3
1.1.3.2 Genetic factors in NTDs	5
1.2 Neural Tube Formation	8
1.2.1 Neurulation in general.....	8
1.2.2 Primary Neurulation	8
1.2.3 Secondary Neurulation	12
1.2.4 Neurulation in Zebrafish	15
1.3 Wnt signaling pathways	15
1.3.1 Canonical/ β -catenin Wnt pathway.....	16
1.3.2 Non-canonical Wnt pathways.....	17
1.3.2.1 The planar cell polarity (PCP) pathway.....	17
1.3.2.1.1 PCP members.....	17
1.3.2.1.2 PCP and convergent extension.....	18
1.3.2.1.3 PCP signaling and ciliogenesis.....	18
1.3.2.2 Wnt/ Ca^{2+} pathway.....	19
1.4 Protein Tyrosine Kinase 7.....	21
1.4.1 The structure of Protein Tyrosine Kinase 7.....	21
1.4.2 The expression pattern of <i>Ptk7</i> during embryonic development.....	22
1.4.3 PTK7 and NTDs.....	23
1.4.4 PTK7 and the Wnt pathways.....	24
1.4.5 <i>PTK7</i> and other related genes.....	26
1.5 The Zebrafish Model for studies of convergent extension.....	27
1.5.1 Advantages of the zebrafish model.....	28
1.5.2 CE in zebrafish	29

1.5.2.1 PCP genes and convergent extension in zebrafish	31
1.5.2.2 Other genes mediating convergent extension in zebrafish.....	33
1.5.2.3 <i>PTK7</i> and CE in zebrafish.....	33
2 Research Project.....	34
2.1 Rationale and significance.....	34
2.2 Hypothesis and objectives.....	34
2.3 Material and Methods	35
2.3.1 Patients and controls.....	35
2.3.2 Re-sequencing of <i>PTK7</i>	37
2.3.3 Genetic validation of rare <i>PTK7</i> mutations	37
2.3.4 Pathogenic Effect Prediction using bioinformatics	37
2.3.5 Expression constructs.....	38
2.3.6 In vitro transcription.....	39
2.3.7 Zebrafish Maintenance, mRNA and Morpholino Injection	40
2.3.8 Statistical analyses.....	40
2.4 Results and Discussion.....	42
2.4.1 Results.....	42
2.4.2 Discussion.....	47
2.4.3 Conclusions.....	49
2.4.4 Future directions.....	50
2.4.4.1 Functional validation of <i>PTK7</i> variants identified in NTDs.....	50
2.4.4.2 Identifications of more genes predisposing to NTDs.....	50

List of the tables

Table 1: Characteristics of the 473 NTDs patients.....	36
Table 2: Primers for sequencing of <i>hPTK7</i>	38
Table 3: Primers for cloning and mutagenesis	40
Table 4: Rare single nucleotide variants identified in <i>PTK7</i> in NTDs.....	45

List of figures

Figure1: Representative NTDs and their defective sites in neural tube closure.....	2
Figure2: Transverse sections for neural tube formation.....	10
Figure3: Schematic diagram of cytoskeleton rearrangements in neural tube formation.....	12
Figure4: Schematic diagram of secondary neurulation.....	14
Figure5: Schematic diagram of neurulation in zebrafish.....	16
Figure6: Schematic model of Wnt pathways.....	20
Figure7: Schematic diagram for convergent extension.....	21
Figure8: The structures of the <i>PTK7</i> gene and its encoded protein.....	22
Figure9: Diagram for convergent extension of zebrafish during gastrulation.....	31
Figure10: Diagram for distribution of the six rare variants identified in <i>PTK7</i> in NTDs and partial alignments of <i>Ptk7</i> orthologues among varies species.....	43
Figure11: Functional validation results of six rare variants in zebrafish.....	46

List of abbreviations

APC	Adenomatous polyposis coli
BMP	Bone morphogenetic proteins
CE	Convergent extension
CK1	Casein kinase 1
Crc	Circle tail
Dgo	Diego
Dkk1	Dickkopf1
DSH (Dvl)	Dishevelled
EMT	Epithelial-mesenchymal transition
FGF	Fibroblast growth factor
Fmi	Flamingo
GSK3	Glycogen synthase kinase 3
<i>Kny</i>	<i>Knypek</i>
Lp	Loop tail
LRP6	Low density lipoprotein receptor-related protein 6
MDCK	Madin-Darby canine kidney
MET	Mesenchymal–epithelial transition
MO	Morpholino oligomers
MT1-MMP	Membrane type 1-matrix metalloproteinase 1
NTDs	Neural tube defects
PCP	Planar cell polarity

pMLC	Phospho-Myosin Light Chain
pk	prickle
<i>ppt</i>	<i>pipe tail</i>
PTK7	Protein tyrosine kinase 7
rMLC	Regulatory myosin light chain
ROCK	Rho-associated protein kinase
<i>slb</i>	<i>silberblick</i>
SHH	Sonic hedgehog
TCF/LEF	T-cell factor-1/ lymphoid enhancing factor-1
TGF	Transforming growth factor
<i>tri</i>	<i>trilobite</i>

Acknowledgements

I would like to give my great appreciation to my advisor Zoha Kibar for her kind and patient help and direction.

I thank all participants in the study and appreciate the help of our colleagues for collecting the samples.

I thank my lab mates for helping me a lot and making research so much fun together.

I would also like to thank the team of Dr. Pierre Drapeau for training me in zebrafish experiments.

1. Introduction

1.1 Neural tube defects

1.1.1 Classification and clinical symptoms

Neural tube defects (NTDs) are among the most common congenital defects of the central nervous system, affecting 1-2/1000 births. They are caused by complete or partial failure of the closure of the neural tube during neurulation [1]. NTDs comprise a wide array of morphologically distinct malformations. There are two types of NTDs according to the morphological appearance at birth. Open NTDs of which the brain and/or spinal cord are exposed and include anencephaly, craniorachischisis, encephalocele, anencephaly and spina bifida. In closed NTDs, the spinal defects are covered by skin and include lipomeningocele and tethered spinal cord. Within these distinct morphologically classified malformations, the clinical syndromes vary from mild to severe such as stillborn or immediate death after birth [2, 3]. The following paragraph will discuss mainly the most common NTDs with their corresponding clinical symptoms. NTD happens following failure of neural tube closure. In both humans and mouse models, there exist multiple neural closure sites. The number and sites of neural tube closure in humans are not as clear as in mouse models [4].

Anencephaly is a severe NTD resulting from failure of complete closure of the rostral end of neural tube during the third to fourth week of conception. It is characterized by absence of telencephalon and the exposure of the residues of brain tissue without the cover of skin and skull (Fig. 1B). The affected babies are unconscious due to the absence of the telencephalon which is responsible for cognition and they cannot survive for long after birth. It is estimated to have an occurrence about 1 in 10000 births in the United States. Due to the fact that many of these pregnancies result in miscarriage, this number might be underestimated [5]. Females babies are reported to be more affected than males [6].

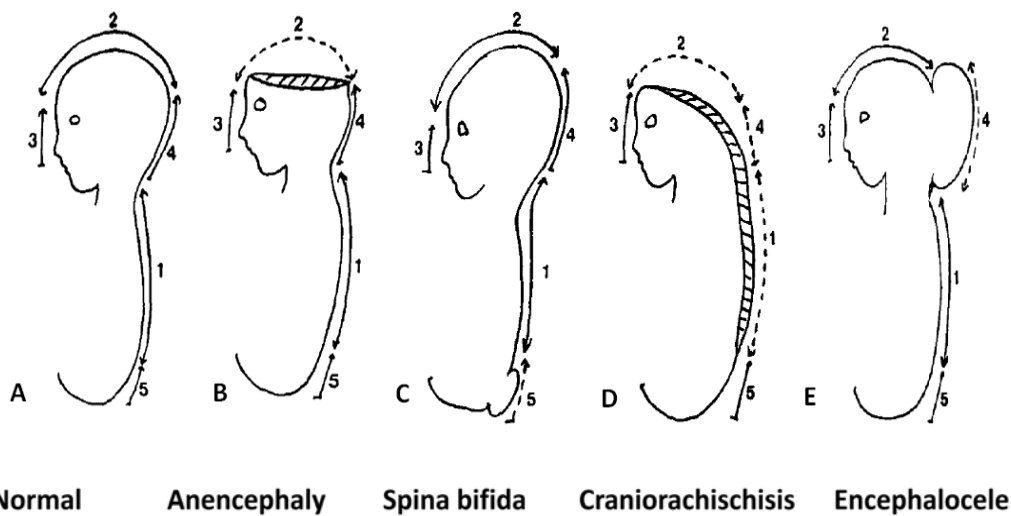


Fig. 1. Representative NTDs and their defective sites in neural tube closure. A: Normal neural tube formation marked with 5 closure initiating sites. B: Anencephaly due to the failure of closure site 2. C: Spina bifida due to the failure of closure site 5. D: Craniorachischisis due to the failure of closure site 1. E: Encephalocele due to the failure of closure site 4 (it also can be due to defect of the closure site 2 or 3 and have this sac-like protrusion at different region). Adapted from Van allen et al, 1993 [7].

Myelomeningocele also known as **spina bifida** affects the posterior region of the spinal cord (Fig.1 C). It is characterised by the opening of spinal cord mainly in the lumbar and sacral regions to varying extents. The clinical symptoms vary and include leg weakness and paralysis, orthopedic abnormalities and bladder and bowel control problems [8].

Craniorachischisis is characterized by an open neural tube in both cranial and spinal regions all along the body axis (Fig.1 D). It is the most severe type of NTDs with a relative low prevalence leading to invariable death at birth [9].

Encephalocele is characterized by sac-like protrusions of the brain and the membranes that cover it through openings in the skull (Fig.1 E). The protrusion can happen in different regions along the cranial and forehead line. The clinical symptoms may include neurological

problems, hydrocephalus, spastic quadriplegia, microcephaly, ataxia, developmental delay, vision problems, mental and growth retardation, and seizures.

1.1.2 The epidemiology of NTDs

NTDs have a world average prevalence of 1-2 per 1000 live births. The prevalence varies between different populations and different geographic regions. For example, the NTD prevalence is as high as 138.7 per 10,000 births in some areas in Shanxi province located in North China [10]. In England and Wales, the NTD prevalence declined from 5-6 per 1000 live birth in the 1950s to less than 1 per 1000 live birth in the 1990s due mainly to the increase in dietary folate intake and to peri-conceptional supplementation with folic acid [11]. The same declining trend was also demonstrated in North America [11]. Recurrence risks among women who have had an NTD-affected pregnancy are markedly higher (5%) than that in the first affected pregnancy in the general population (0.2%). And the risk would go up to 10% for the third pregnancy and 28% for the fourth pregnancy [12]. Concordance rates of monozygotic twins (7.7%) for NTDs exceeds that of dizygotic twins (4.0%) suggesting a genetic contribution [12].

1.1.3 Aetiology of NTDS

The etiology of NTDs is complex involving environmental and genetic factors as suggested by epidemiological studies and genetic studies mainly conducted in animal models. Environmental factors associated with NTDs include folic acid insufficiency during the pregnancy, maternal obesity, maternal hyperinsulinemia and hot water exposure in the first trimester. Previous pregnancy wastage and family history of NTDs are also considered as risk factors for NTDs [11]. Here, I will mainly discuss the role of folic acid in protection against NTDs and the genes associated with NTDs to date.

1.1.3.1 Folic acid

Folic acid (folate) is a form of the water-soluble vitamin B9. After absorption, it acts as an acceptor or donor of one-carbon units in a variety of reactions involved in amino acid and nucleotide metabolism, which is important for methylation, DNA synthesis and cell division.

A severe folic acid deficiency causes the macrocytic megaloblastic anemia characterized by many large immature and dysfunctional red blood cells in the bone marrow [13].

The relation of folic acid to NTDs was revealed by epidemiological studies where it was confirmed that peri-conceptional intake of folic acid decreases both the recurrence rate among pregnancies following an NTD-affected pregnancy and the occurrence rate in the general population [14]. It has been estimated that around 70% of human NTDs are preventable by adequate folate intake [15, 16]. Daily intake of 0.8 mg of folic acid as a vitamin supplement by pregnant women shows a significantly decreased occurrence of NTDs as compared to the control population (NTD cases in the number of pregnancies: 0 in 2420 versus 6 in 2333 with and without folate supplementation respectively in Caucasians [14]).

The protective effect of folic acid against NTDs was confirmed by many subsequent observations or/and interventions conducted in distinct regions in the world. A study conducted in 1999 in China confirmed this preventive effect and at the same time showed that this effect is more marked in the region with high prevalence of NTDs than in the region with lower prevalence [17]. Food fortification is the practice of adding essential vitamins and minerals to staple foods to improve their nutritional content. A study conducted in Canada also showed that the prevalence of spina bifida decreased from 0.86/1,000 in the pre-fortification to 0.40 in the full fortification period [18].

Despite a well established protective effect of folate against NTDs, the underlying mechanisms remain unclear. Metabolic abnormalities of folic acid were suggested as one of the possible mechanisms as studies demonstrated a link between levels of maternal plasma and/or red cell folate level, plasma Vitamin B12, plasma Vitamin C (both are involved in the metabolism of folic acid), homocysteine and the risk of having fetuses affected with NTDs [19-24]. A study conducted on 81 women carrying NTD-affected fetuses during their pregnancies and 247 women carrying normal fetuses showed that both plasma folate and B12 levels were significantly lower in women who were carrying affected fetuses than in controls [20]. The prevalence decreased from 6.6 per 1000 births in women whose red cell folate levels

were below 150 ng/ml (340 nmol/l) to 0.8 per 1000 births in women whose red cell folates were over 399 ng/ml (906 nmol/l) [21]. Homocysteine can be transformed to methionine with the help of Vitamin B12 while the 5-Methyl tetrahydrofolic acid (5-MTHF) is transformed to tetrahydrofolic acid (THF) in the same reaction. The relation of homocysteine with NTDs was first indicated where mothers of NTDs-affected children tended to have higher total plasma homocysteine as compared to controls with no NTD-affected children in the methionine loading test [22]. Higher amniotic fluid total homocysteine was also detected in the NTD case mothers and not in controls [23]. These results were further confirmed in pregnant woman carrying NTDs affected children and controls [24].

All these studies provide strong evidence for defects in the metabolism of folic acid in NTDs. Consequently, folate-related genes were investigated for involvement in NTDs by direct re-sequencing and association studies. The variant c.677C→T detected in 5,10 methylenetetrahydrofolate reductase (MTHFR) that catalyzes the essentially irreversible conversion of 5,10-methyleneTHF to 5-methylTHF was the first folate-related genetic factor reported to be associated with NTDs. It was shown that homozygous TT individuals carry a mildly higher plasma homocysteine concentration [25]. The T variant results in an enzyme that binds its cofactor flavin adenine dinucleotide (FAD) with lower affinity than the C variant. This affinity reduction can be compensated by addition of the cofactor FAD or by addition of folate, which explains why the elevated homocysteine levels seen in individuals homozygous for the TT variant can be partially reversed by riboflavin intervention [26-28]. Many genetic studies were conducted to find candidate variants in folate related genes, but the results were not as exciting as the original ones with many conflicts between different reports [29]. Clearly, additional studies are needed to better understand the relationship of folic acid metabolism and the occurrence of NTDs.

1.1.3.2 Genetic factors in NTDs

The evidence from epidemiological studies suggests a strong genetic contribution to the etiology of human NTDs [12]. Concordance rates of monozygotic twins (7.7%) for NTDs exceeds that of dizygotic twins (4.0%) [30].

The genetic contribution is also supported by the fact that NTDs are a feature (or symptom) of known genetic syndromes, such as trisomy 13, trisomy 18, and Meckel-Gruber syndrome [31]. Despite the strong evidence for a genetic component in NTDs, the major associated gene(s) or pathways have not been determined yet, mainly due to the complexity of the NTDs' etiology. At the same time, with the dramatic improvement in ENU (N-ethyl-N-nitrosourea) mutagenesis and other transgenic techniques, many NTDs-related genes were identified from genetic studies conducted in mouse models [4]. These genes are involved in regulation of actin dynamics, cell adhesion, electron transport, DNA damage repair, and other processes [32, 33]. I will present a few examples of NTD genes identified in mouse models focusing mainly on planar cell polarity genes and their possible upstream and downstream effectors.

The Loop-tail mouse is a well established mouse model for NTDs and is characterized by a looped tail phenotype in heterozygous mice, and craniorachischisis in homozygous embryos. The gene defective in Lp was identified as *Vangl2* and is a mammalian ortholog of the *Drosophila* gene *stbm/vang* that forms part of the planar cell polarity (PCP) pathway controlling the convergent extension (CE) process in vertebrates which will be discussed later in section **1.3.2.2**. Lp was the first mouse model to implicate PCP signalling in the pathogenesis of NTDs [34]. Since this study, many other mouse NTD mutants with PCP genes including *Frizzled1*, *Frizzled3*, *Celsr1*, *Scribble1*, *Dishevelled1*, *Dishevelled3*, and *Protein tyrosine kinase7*, were identified and showed various degrees of genetic interaction among them in the incidence of NTDs, confirming an important role of PCP signalling in development of NTDs [35-38]. Other potential downstream effectors of PCP signalling were also shown to cause NTDs in mice like Rho [39].

Canonical Wnt/ β -catenin pathway and the non-canonical Wnt/PCP pathway together regulate a lot of developmental processes including convergent extension. *Dishevelled* (*Dsh*), *axin*, and *glycogen synthase kinase 3* (*GSK3*) are involved in both pathways. They are very important in keeping the balance between these two pathways [40].

The human orthologues of PCP genes were investigated for their role in human NTDs by re-sequencing analyses of their coding regions. The first study that aimed at screening *VANGLI* in human NTDs identified 3 novel rare missense mutations in this gene in 3 NTD patients: p. Val239Ile and p.Arg274Gln in 2 familial cases of NTDs and p.Met328Thr in a sporadic NTD case. Subsequent functional validation of these mutations using the yeast two hybrid system demonstrated that p.Val239Ile abolished interaction of Vangl2 with Dishevelled proteins and hence is most likely pathogenic [41]. The two variants p.Val239Ile and p.Met328Thr were also proven to be damaging in a zebrafish model where they failed to rescue a defective CE phenotype in zebrafish embryos injected with a morpholino oligonucleotide directed against *Vangl2* [42]. Following these initial studies, larger studies conducted in larger cohorts of open and closed forms of NTDs have identified additional novel rare missense mutations in *VANGLI* or *VANGL2* associated with NTDs thereby confirming their role in these malformations. For *VANGLI*, 7 patients were heterozygous for 5 novel missense mutations, two of which, p.Ser83Leu and p.Arg181Gln, occurred in familial settings. Four mutations, p.Phe153Ser, p.Arg181Gln, p.Leu202Phe and p.Ala404Ser, were “private” and one mutation, p.Ser83Leu, was recurrent in 3 familial cases of tethered cord syndrome [43]. For *VANGL2*, six novel rare missense mutations were identified in 7 patients which are absent in the controls, five of which were detected in closed spinal NTDs [44].

A study of another PCP gene, *PRICKLE1*, in the same cohort used in the above mentioned studies identified 7 rare missense heterozygous mutations that were absent from controls. Functional validation in zebrafish has demonstrated that one variant; p.Arg682Cys antagonized the CE phenotype induced by the wild-type zebrafish *prickle1a* in a dominant fashion [45]. Other PCP genes including *CELSRI*, *FRIZZLED 6*, *DVL1* and *DVL3* were also demonstrated to be associated with NTDs in a small fraction of patients. All these studies taken together confirm an important contribution of PCP genes to the occurrence of human NTDs.

CE is a process which is governed by many signalling pathways including PCP. The detailed morphological or molecular changes that occur in this process will be discussed later in section 1.3.2.2. To better understand the association of PCP genes with NTDs, I will describe the normal neural tube formation in the following section.

1.2 Neural Tube Formation

1.2.1 Neurulation in general

Neurulation is an embryonic process by which the neural tube is transformed into the primitive structures that will later develop into the central nervous system. Neurulation in mammalian embryos occurs in two phases: primary and secondary neurulation [46]. These two phases occur in distinct areas along the rostro-caudal axis of the embryo. Primary neurulation happens on most of the axis from rostral end to the tail bud while the secondary neurulation is limited to the tail bud, which lies beyond the caudal neuropore. Primary neurulation occurs during the third and fourth weeks of pregnancy. It is the process by which the neural plate folds into the cylindrical neural tube leading to the formation of the brain and most of the spinal cord. Secondary neurulation occurs during the fifth and sixth weeks of pregnancy. It is the process by which mesenchymal cells in the dorsal part of the tail bud undergo condensation and epithelialisation (MET, mesenchymal–epithelial transition) to form the secondary neural tube which in turn forms the lowest portion of the spinal cord including most of the sacral and all the coccygeal regions [47]. The lumen of the secondary neurulation is continuous with that of the primary neural tube.

1.2.2 Primary Neurulation

Primary neurulation can be subdivided into several stages: induction and formation of the neural plate, formation and elevation of the neural folds and closure of the neural groove (Figure 2) [48]. In each of these stages, specific tissue changes and specific molecules or genes are involved. Induction of the neural plate is mediated by some molecules secreted by primitive node that include Noggin, Chordin, Cerberus, Xnr3, Follistatin, Frzb, and eFGF [49]. These molecules suppress the default epidermal fate of the naive neural ectoderm by inhibiting

the BMPs and Wnts signals. After the induction, the formation of the neural plate is autonomous without the signalling from the surrounding epidermal ectoderm [50]. Then the neural plate conducts a CE morphogenetic process to narrow and elongate the neural axis in the mediolateral and rostro-caudal axes. This process will be discussed in detail in Section 1.3.2.2. At the same time the neural progenitor cells in the neural plate undergo apical constriction that would lead to changes in cell shape from cuboidal to columnar and finally to wedge- or bottle-like while the cell volume keeps constant [51, 52]. Combining with the extrinsic forces generated by the CE movement in non-neural ectoderm, the intrinsic forces generated from the shape change initiate the bending of the neural plate [53, 54]. A groove is formed during this bending and finally develops the lumen of the neural tube after its closure. After its closure, the neural tube is separated from the overlaying epidermal ectoderm, which will further develop in to the skin of the back of the embryo. At this stage, another important cell population called neural crest cells and located between the neural tube and the epidermal ectoderm starts to migrate and finally develops into various tissues in different structures [48].

Closure of the neural tube groove is initiated at some specific sites and then elongates uni-directionally or bi-directionally to meet with the elongation from another site leading to complete closure of the whole neural tube. It is well established that there are multiple initiation sites for neural tube closure in both humans and mouse models, but the exact number of these sites is still undefined [4, 7]. For example in mouse models, 3 main distinct initiation sites along the neural axis are thought to function in a temporal and spatial-specific pattern to complete neural tube closure while in humans there are probably 5 sites [7]. Defects happening in these different initiation sites or in the elongation region of these sites will result in various NTD types [1, 7]. The representative NTDs and the corresponding closure defects are shown in Fig1.

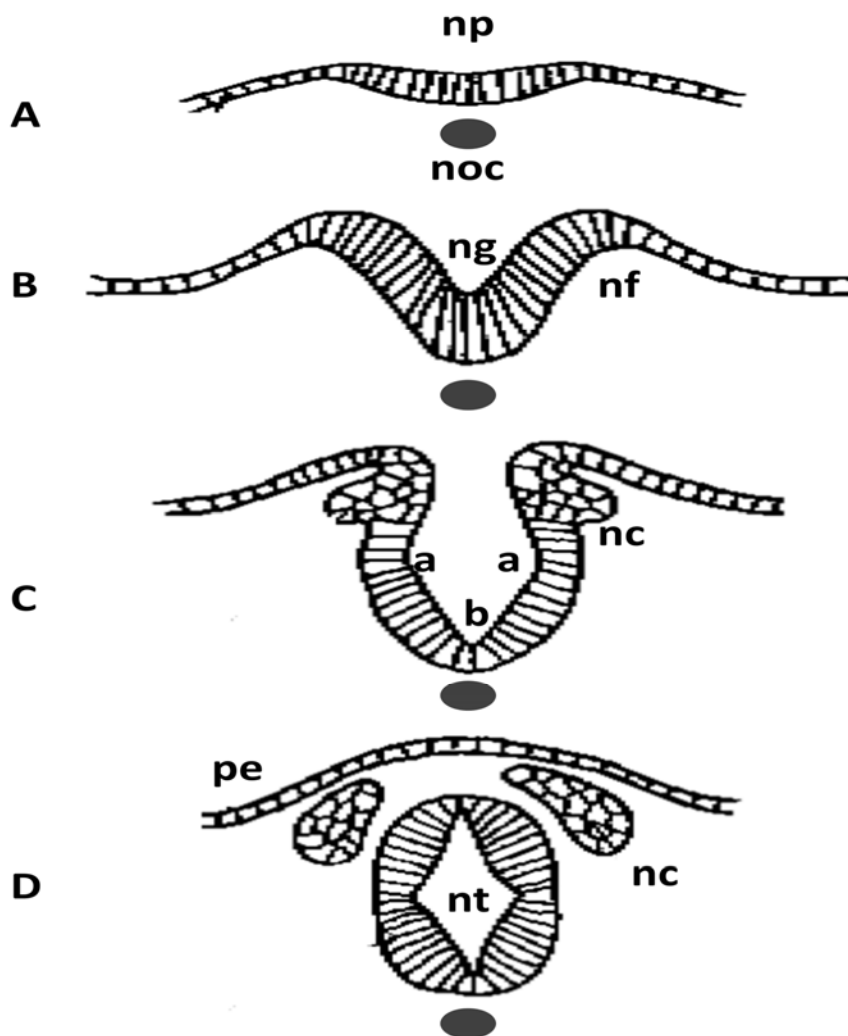


Fig. 2. Transverse sections for neural tube formation. Neural plate is induced by notochord under it (A). Neural folds form and elevate to create the neural groove (B). Bending or hinge points form at two sites: the dorsolateral hinge points (a) at the lateral extremes of the neural plate and the median hinge point (MHP) (b) overlying the notochord. With continued bending, the neural tube is closed and separates from the presumptive epidermis while the neural crest form and migrate to lateral sides. noc, notochord; np, neural plate; nf, neural fold; ng, neural groove; nt, neural tube; nc, neural crest; pe, presumptive epidermis.

Adapted from <http://instruct.uwo.ca/anatomy/530/anfound.htm>.

The major morphogenetic changes in cell shape or movement are caused by cytoskeletal rearrangements (Fig.3). Actin filaments (F-actin) constitute a major component of the cytoskeleton that is composed of monomeric actin (G-actin). It is present at the apical junction of the neural plate cells in the form of circular bands. During the neural tube closure process, the band thickens leading to apical constriction (Fig. 3C) [55, 56]. Another essential cytoskeletal component is myosin II that also contributes to the apical constriction [57]. Myosin II is composed of two heavy chains, two essential light chains and two regulatory light chains. The activity of myosin II is regulated through phosphorylation of its regulatory light chain (rMLC) mainly by Rho-associated kinase (ROCK), an effector of the small GTPase Rho. Myosin II is co-localized with F-actin in the apical side of neural plate cells (Fig. 3C) [58]. Either the disruption of F-actin or inhibition of Myosin II activity can cause the disappearance of the apical constriction and failure of neural tube closure in chick embryos [39, 56, 58]. This causative relationship was also observed in *Xenopus* in which the expression of myosin II was reduced by a morpholino oligonucleotide (MO) leading to failure of the F-actin accumulation and apical constriction [58]. Microtubules are involved in the cell elongation during the neurulation process. Consistent with the shape changes of the neural plate cells from cuboidal to columnar; the microtubules are reorganized from random distribution and disorientation throughout the cells to a parallel orientation to the axis of elongation (Fig. 3A, B, C) [56, 59]. It was shown that the neuroepithelial cells treated with microtubule polymerization inhibitors prior to the elongation process failed to elongate in chick embryo. In *shroom3* mutants and MO-injected embryos, apical constriction is significantly inhibited, associated with a severe reduction in apical accumulation of F-actin and phosphorylated MLC (pMLC) [60]. In addition to intracellular molecules, cell adhesion molecules such as N-cadherin and nectin-2 also play crucial roles in cellular morphogenesis during neural tube closure (Fig. 3C). All these studies demonstrate that cytoskeletal rearrangements generate the driving force for shaping the neural plate cells and closure of the neural tube. The molecular mechanisms involved in these rearrangements still remain poorly defined.

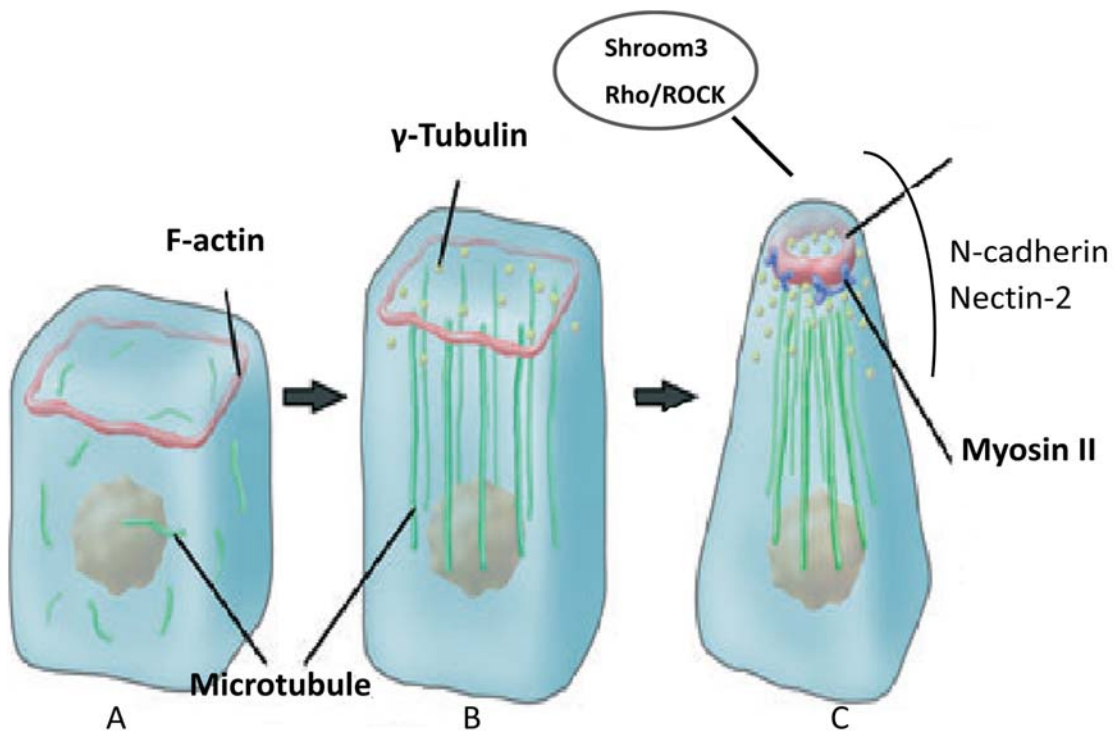


Fig. 3. Schematic diagram of cytoskeleton rearrangements in neural tube formation. In cuboidal neuroepithelial cells prior to neurulation (A), F-actin exists in a thin circular band (red) at apical junction, while microtubules (green) are diffusely distributed in cytoplasm. During cell elongation, non-centrosomal γ -Tubulin particles (yellow) are distributed apically while microtubules polymerize and assemble parallel to the apicobasal axis (B). During apical constriction, actin filament bands constrict and become thickened. Non-muscle myosin II (green) actively slides and generates contractile force along apical actin filaments. The molecules that are accumulated at the apical junctions are shown in the circle while the adhesion molecules crucial for this constriction are marked besides. Adapted from Suzuki M et al, 2012 [60].

1.2.3 Secondary Neurulation

Secondary neurulation is initiated immediately after completion of the primary neurulation in the most posterior part of the caudal axis. Distinct from the primary neurulation, there is no neural plate formation or neural folds elevation. As indicated in Fig. 4, the bilateral

mesenchymal cells under the epithelial ectoderm undergo a mesenchymal-to-epithelial transformation (MET) characterized by a series of changes in the cell surface oligosaccharide complement of the differentiating cells. These cells together with the undifferentiated central mesenchymal cells migrate at the same time to form the cell mass located in the midline [61]. This is followed by formation of small cavities at the boundary between the two cells' populations. These cavities enlarge while the central cells intercalate with the peripheral cells, and merge with each other resulting in a single lumen which becomes continuous with the neurocoele of the primary neural tube [61]. Developmental defects in this process are associated with closed spina bifida where the developing neural tube fails to separate from other tissues of the tail bud [62].

MET is the reverse process of epithelial–mesenchymal transition (EMT). Unlike epithelial cells which are stationary and characterized by an apical-basal polarity, tight junctions, and expression of cell-cell adhesion markers, mesenchymal cells do not have these mature cell-cell contacts and can invade the extracellular matrix. This transformation is very well studied in kidney ontogenesis, somitogenesis and cancer. The mechanisms by which the mesenchymal cells conduct this transformation are unknown. Some changes in gene expression patterns were reported during this transformation [63]. For example, *Sox2* expression is not detected in the mesenchymal cell mass at the beginning of secondary neurulation and become detectable at later stages in a cell cluster in the medullary cord which is the precursor of the neural tube. A similar pattern was observed for other epithelial apical-basal polarity markers such as laminin and fibronectin (basal markers), N-cadherin and atypical protein kinase C (aPKC) (apical markers). At the same time, it was shown that these markers also propagate in dorsal to ventral orientation [63]. Activity levels of Rho family GTPases Rac1 and Cdc42 were also shown to be critical for the MET during secondary neurulation.

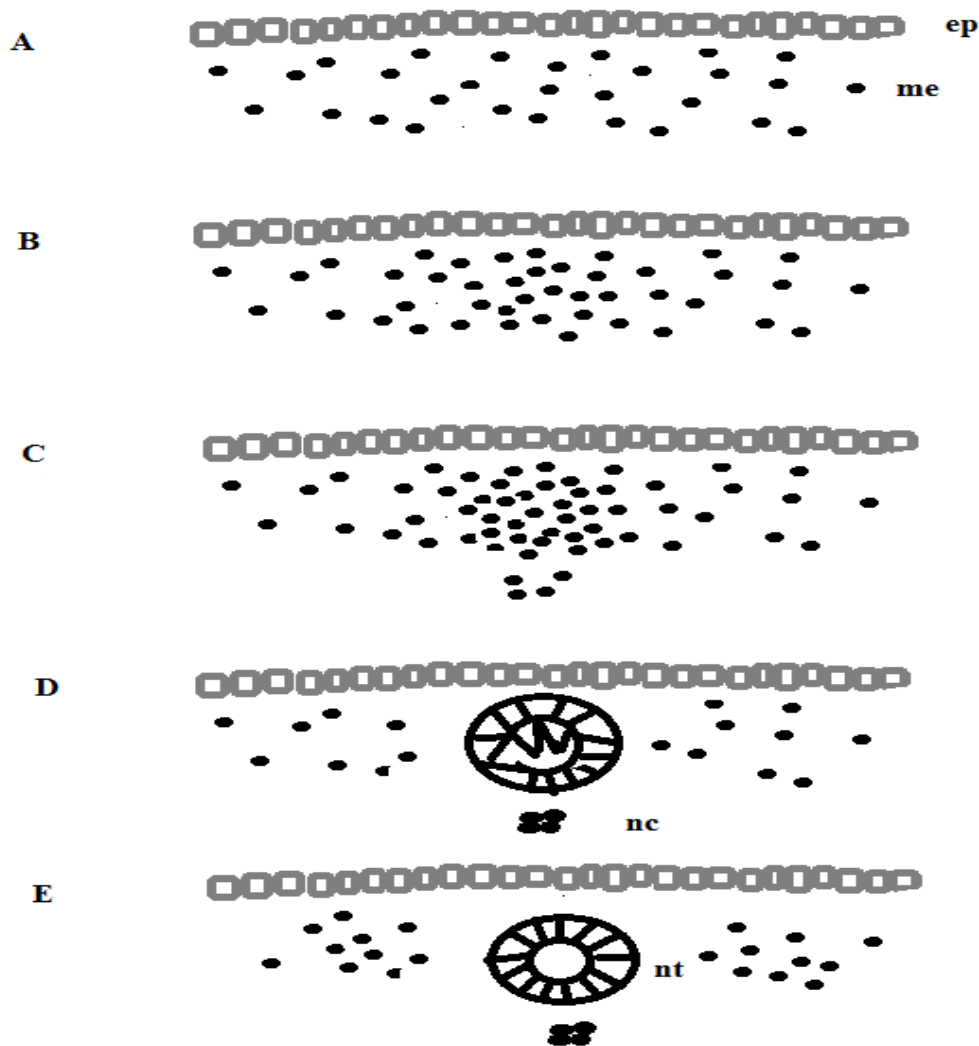


Fig. 4. Schematic diagram of secondary neurulation. The bilateral mesenchymal cells under the epithelial ectoderm (A) proliferate, migrate and finally condensate at the midline (B, C). The condensed mesenchymal cells undergo MET and transformed to be neural epithelial cells (D). At the same time, small cavities starts to form inside the cell mass (D). Finally the neural tube lumen formed with the complete neural epithelial cells transformation (E). me, mesenchymal cells. ep, epithelial cells. nt, neural tube. nc, notochord. Adapted from: <http://scienceblogs.com/pharyngula/2008/01/02/neurulation-in-zebrafish/>.

1.2.4 Neurulation in Zebrafish

As zebrafish (*Danio rerio*) will be used in our study as an animal model, I will point out some specific characteristics of the neurulation process in zebrafish. Neurulation in zebrafish tail is conducted through secondary neurulation as in other vertebrates. Whether the neurulation in the head and trunk (Fig. 5) goes through primary or secondary neurulation is still in dispute. The process of this neurulation does not start from the condensation of mesenchymal cells in the midline as in traditional secondary neurulation. Instead, it starts from the columnarization of neural plate cells. A solid neural keel is formed by the accumulation of these columnarized neural plate cells. A solid neural tube (neural rod) will be formed following the separation of the neural keel from the originating neural plate. The lumen will appear after the solid neural tube goes through the cavitation process [64].

1.3 Wnt signalling pathways

The Wnt members are secreted glycoproteins which can bind to different membrane-anchored receptors to activate multiple important pathways including canonical and non-canonical signalling pathways. The determinant of which pathway will be activated has been recently suggested to be the different Wnts and different co-receptor crossbinding [65]. Wnt signalling functions in cell proliferation, stem cell maintenance and cell fate decisions, as well as organized cell movements and the establishment of tissue polarity in one layer. It is also known to be related to human cancers and degenerative diseases, mainly by activation of canonical and non-canonical Wnt pathways [65].

The NTD phenotypes were observed in mouse mutants of genes involved in canonical (*Wnt3* and *Lrp6*) as well as non-canonical Wnt signalling (*Vangl2* and *Ptk7*) [66]. This suggests that the balance between these two pathways is very critical to the neurulation process.

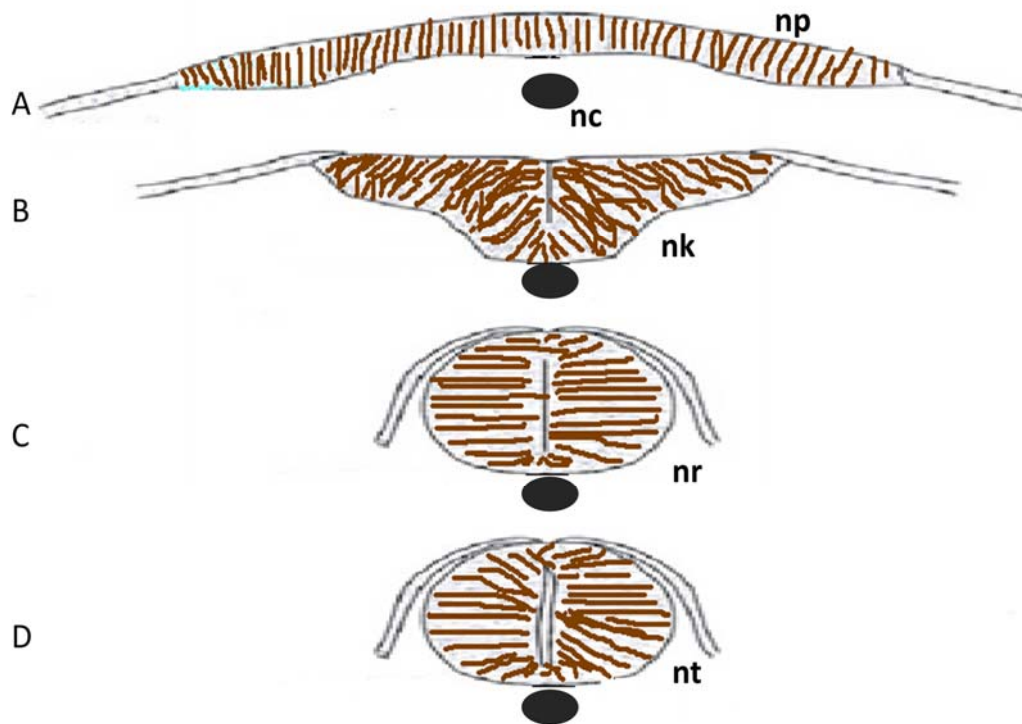


Fig. 5. Schematic diagram of neurulation in zebrafish. The neural plate folds inward at the midline (A,B) and form the neural keel, the keel progressively rounds up, forming the neural rod (C) without a lumen inside while the cells from lateral fuse to form the epidermal layer . Cavitation starts from the ventral side of the neural tube to the dorsal side finally forming the neural tube (D). np, neural plate; nc, notochord; nk, neural keel; nr, neural rod, nt, neural tube.

Adapted

from: <http://scienceblogs.com/pharyngula/2008/01/02/neurulation-in-zebrafish/>.

1.3.1 Canonical/ β -catenin Wnt pathway

The core member in the canonical Wnt pathway is β -catenin, which is constantly synthesized and then degraded through phosphorylation and ubiquitination by a so-called destruction complex consisting of the scaffolding protein Axin, APC (adenomatous polyposis coli), GSK3 (Glycogen synthase kinase-3) and CK1 (casein kinase 1) (Fig. 6) [67]. Without the stimulation by Wnts, β -catenin is constantly degraded by this destruction complex. Once

the appropriate Wnt like Wnt3 or Wnt8 binds to the right Frizzled receptor, with the presence of other co-receptors like Lrp5/6 (low density lipoprotein receptor 5 or 6), Dsh is recruited to the membrane followed by its phosphorylation and this leads to disassembly of the destruction complex. β -catenin is then released from the complex, accumulates in the cytoplasm and then translocates into the nucleus. By relieving TCF/LEF (T-cell factor/Lymphoid enhancer-binding factor) from binding with transcription repressor Groucho, Wnt functions as a transcriptional activator and targets gene expression [65]. Canonical Wnt/ β -catenin pathway is proven to function in cell proliferation, stem cell maintenance and cell fate decisions [68]. Defects in this pathway are responsible for tumorigenesis and developmental defects. β -catenin was found to be mutated and causing hyperactivation of Wnt/ β -catenin signalling in virtually all intestinal cancers and other malignancies. In *Drosophila*, the mutation of *Wnt1* homolog *Wingless* causes a segment polarity defect [66, 69].

There are disputed findings about the direct stream of Wnt, β -catenin, TCF/LEF, target gene activation pathway [70]. For example, TGF- β can also regulate the nucleus translocation of β -catenin independent of Wnts. Blocking the transcription activity of TCF could not block all the phenotypes induced by canonical Wnt ligands indicating another branch of downstream effectors besides TCF/LEF [70]. However, another group show that a dominant negative form of TCF4 abrogates DNA recruiting by any of the known transcription factors [71].

1.3.2 Non-canonical Wnt pathway

1.3.2.1 The planar cell polarity (PCP) pathway

1.3.2.1.1 PCP members

The PCP pathway was first demonstrated in *Drosophila* and is highly conserved in vertebrates [72, 73]. It shares some common members with canonical/ β -catenin Wnt pathway like Fz and Dsh (Fig. 6). Genetic studies of a wide range of mutants affecting some highly organized structures in the fly, like the distal orientation of wing hairs, the posterior orientation of the abdominal bristles and the more complex organization of the ommatidia (eye units) in the adult eye, have identified a group of so-called core PCP genes required for PCP signalling in all tissues and which include: Frizzled (Fz), Dishevelled (Dsh/Dvl),

Strabismus/Van Gogh (Stbm/Vang), Flamingo (Fmi), Prickle (Pk) and Diego (Dgo) [73-75]. In planar cells, PCP members are asymmetrically localized at the cell membrane: Fmi, Fz, Dsh, and Dgo localize to the distal region of the cell, whereas other PCP members Fmi, Vang and Pk localize to the proximal region. After Dsh recruitment to the membrane under the stimulation of some non-canonical Wnt activators (Wnt4, Wnt5a and Wnt11), PCP signalling through unknown mechanisms, lead to activation of the small GTPases RhoA and Rac, resulting in modification of the cytoskeleton like the contraction of F-actin and microtubule reorganization (Fig. 6). This modification ultimately results in the polarization of cells within epithelia and polarized cell migration [75, 76].

1.3.2.1.2 PCP and convergent extension

PCP signalling is essential to a morphogenetic pathway called CE during gastrulation and neurulation in vertebrates. CE is the process by which cells move from the lateral side to the midline and intercalate with each other giving rise to a longer and narrowed anterior – posterior axis (Fig. 7) [65]. CE is a major driving force for neural tube formation and closure. In *Vangl2* mutant Loop tail mice, the NTD phenotype craniorachischisis was demonstrated to be the result of a defective CE process manifested by a shorter anterior-posterior axis and wider left-right axis [77]. These CE defects were also observed in other PCP mutant mice models like Crash (*Celsr1*), *Dvl1/Dvl2* double knockouts, *Fz3/ Fz6* double knockouts, Circle tail (*Scribble1*) and Chuzhoi (*Ptk7*) [32].

1.3.2.1.3 PCP signaling and ciliogenesis

Cilia are microtubule-based protrusions on the surface of most vertebrate cells. There are two types of cilia: motile cilia and non-motile cilia (primary cilium). It is well known that motile cilia beat in coordinated waves to sweep mucus out of the respiratory tract or move the ovum from the ovary to the uterus [78]. The function of primary cilium was first illustrated to be linked to patterning of the mouse embryo by transducing Hedgehog signaling [79]. The mouse mutants show phenotypes characteristic of Hedgehog signaling defects including an open neural tube on the head and preaxial polydactyly. Following this, additional studies confirmed the role of cilium in inducing rostral neural tube defects [80, 81]. In humans, genes

involved in ciliogenesis are proven to be responsible for some Meckel-Gruber syndrome that typically involves meningo-encephalocele, polycystic kidneys and postaxial polydactyly [82, 83]. In contrast to cilia mutants, PCP mutants are more affected with caudal neural tube defects [84]. Inversin, a homolog of the PCP member Diego in fruit fly, was more studied in the context of ciliogenesis and was responsible for some renal cystic diseases [85]. Reduced expression of either PCP effectors Inturned or Fuzzy generated rostral neural tube closure defects [86].

PCP was shown to regulate the orientation of cilium in both individual cells and at the tissue level of radial glial cells and ependyma to create a coordinated beating [87]. Additional studies are needed to better understand the relationship between PCP members and cilium polarity and relationship between PCP members and Hedgehog signaling.

1.3.2.2 Wnt/Ca²⁺ pathway

The Wnt/Ca²⁺ pathway is another major non-canonical Wnt pathway. There is crosstalk between the Wnt/Ca²⁺ pathway and the canonical β -catenin pathway or PCP pathway at different levels [88]. Wnt/Fz ligand receptor binding leads to a transient increase of certain intracellular signaling molecules, inositol 1,4,5-triphosphate (IP3), and 1,2 diacylglycerol (DAG). IP3 causes release of Ca²⁺ from ER (endoplasmic reticulum). Calcium ions in the presence of calmodulin or DAG can activate CaMKII (calcium calmodulin dependent protein kinase II) or protein kinase C (PKC). CaMKII and PKC can activate nuclear transcription factors (NFkB and CREB). Calcium can also activate phosphatase calcinurin (Cn) that can further activate nuclear factor associated with T cells (NFAT) (Fig. 6). These activated nuclear factors will regulate the expression of various genes related to development, cancer, and cellular responses as a consequence of inflammatory challenges. The Wnt/Ca²⁺ signaling pathway was proved to promote ventral cell fate through CaMKII during early embryogenesis in *Xenopus* [89].

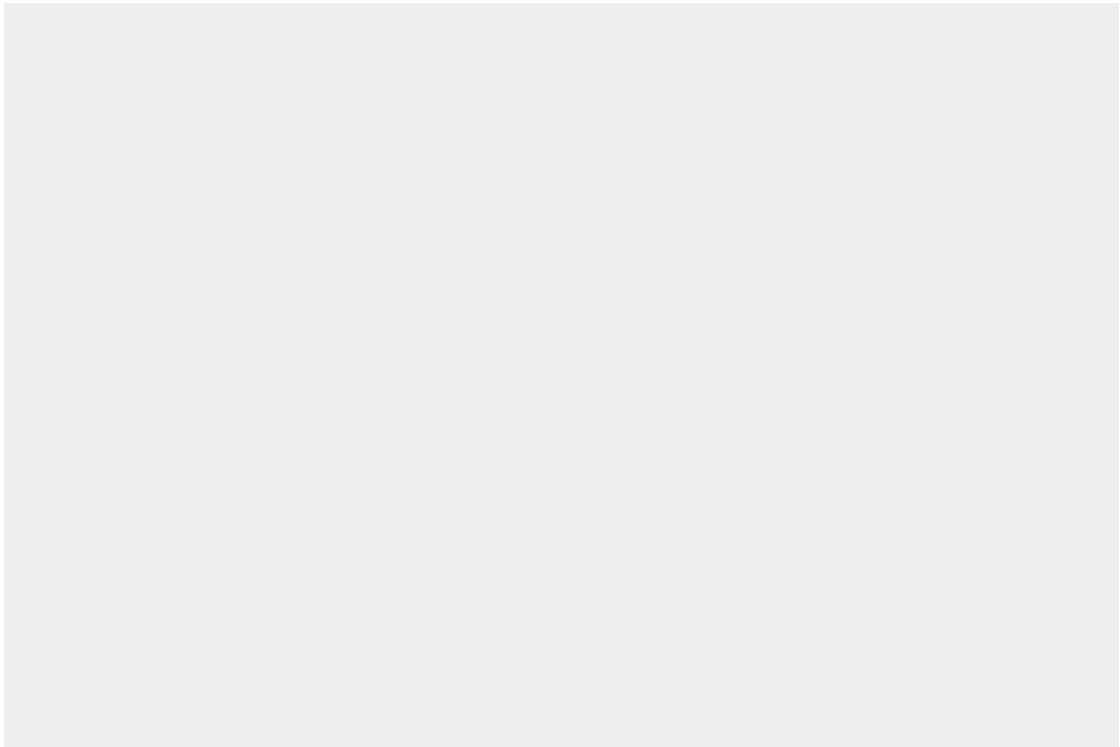


Fig. 6. Schematic model of Wnt pathways. Canonical Wnt ligands bind to the membrane receptor Fzd forming a complex with some known and unknown co-receptors like Lrp5/6. The subsequent Dvl membrane recruitment and interaction with Axin induce the disassembly of the β -catenin degradation complex. The free β -catenin accumulates in the cytoplasm and enters in the nucleus to activate the transcription of canonical target genes via an association with the DNA binding factors LEF/TCF. Non-canonical Wnt ligands bind to Fz with the help of co-receptors and recruit Dvl to the membrane. Small GTPase family members Rac/Rho are activated and regulate the cytoskeletal reorganization. The core PCP members Vangl, Diversin, Prickle, and Ceslr are all involved in the Dvl membrane localization. Diversin at the same time regulates the degradation of β -catenin. Wnt/Fz ligand receptor interaction with co-receptor Ror1/2 leads to the production of IP3 and DAG from phospholipid phosphatidyl inositol 4, 5-bisphosphate (PIP2). IP3 causes release of Ca^{2+} from ER; Cn and CamKII are activated which in turn activate NFAT and NFkB. DAG is activated by released calcium from ER, which activates PKC. PKC activates NFkB and CREB which together with NFAT will regulate downstream gene expression. Dotted arrows show the pathway direction; Green lines show the genetic or physical interaction between two proteins. The red line shows the binding that can inhibit the non-canonical pathway.

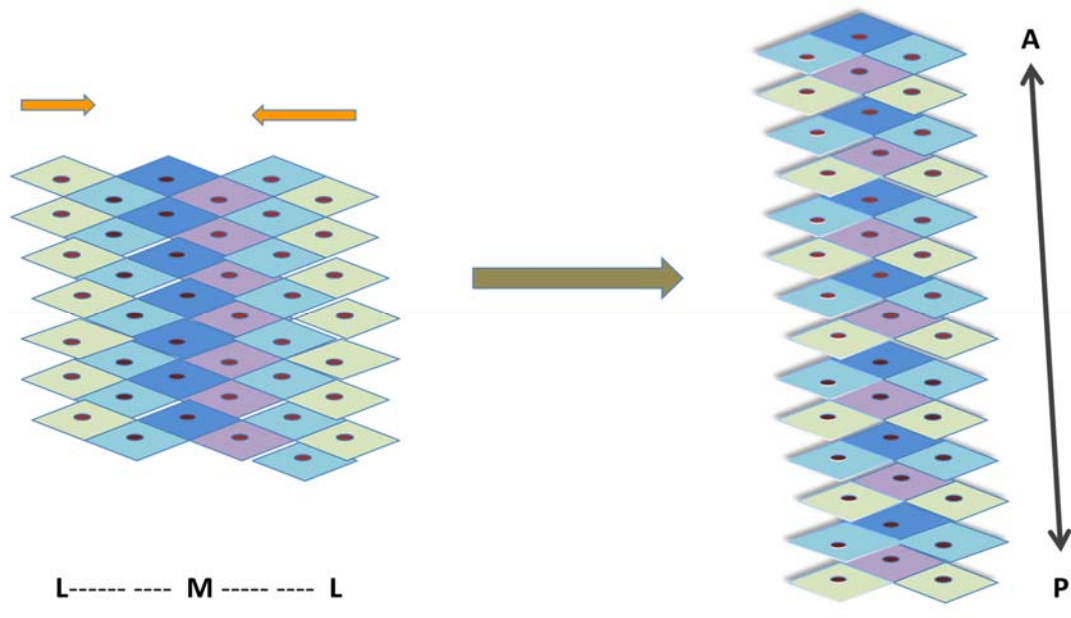


Fig. 7. Schematic diagram for convergent extension. The polarized cells lining the lateral side (green and light blue) migrate to the midline. Cells intercalate to each other resulting in narrowing in the medial-lateral axis and extending in the anterior – posterior axis. M, midline; L, lateral line; A, anterior; P, posterior.

1.4 Protein Tyrosine Kinase 7

1.4.1 The structure of Protein Tyrosine Kinase 7

The first study on *Ptk7* involved the cDNA coding of KLG that is the homolog of *Ptk7* in chicken [90]. Human *PTK7* and mouse *Ptk7* were subsequently cloned [91, 92]. The human *PTK7* gene is located to chromosome 6 and its coding region consists of 20 exons (NCBI Gene ID: 5754; Ensembl ID: ENST00000230419). Among multiple splicing transcripts, the longest isoform encodes a protein composed by 1070 amino acids (Fig. 8, upper panel) [93]. Human *PTK7* is a highly conserved single pass transmembrane protein that consists of one signal peptide which targets the protein to the membrane, seven extracellular Ig-like (immunoglobulin-like) domains and one cytoplasmic tyrosine kinase homolog domain which

lacks kinase activity due to the absence of the DFG triplet which is essential for kinase activity (Fig. 8, lower panel).

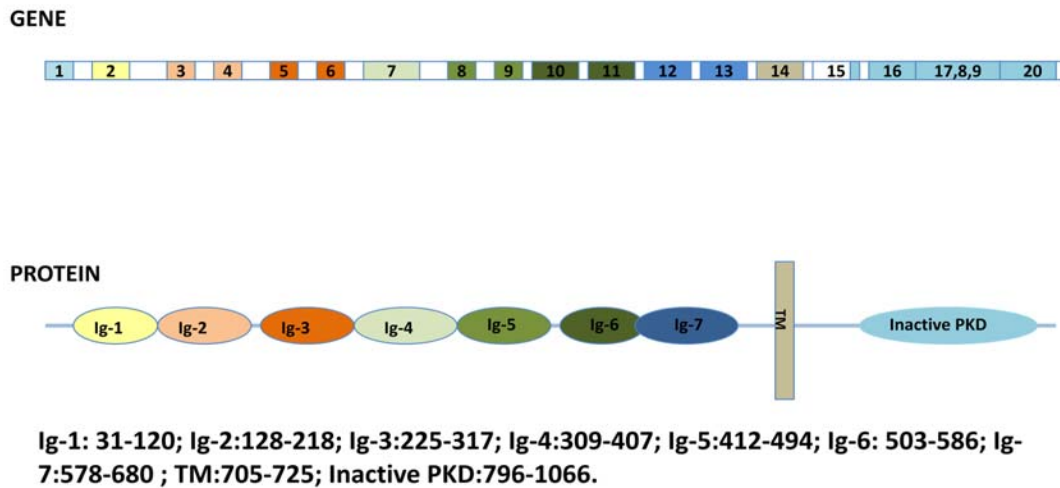


Fig. 8. Schematic digrams of the structures of the *PTK7* gene and its encoded protein. In the upper panel, each square stands for one exon where a different color is consistent with the domain that it codes for. On the lower panel, each oval stands for one domain whereas the TM domain is marked by a grey column. TM, transmembrane; Ig, immunoglobulin-like; Inactive PKD, inactive protein tyrosine kinase domain.

1.4.2 The expression pattern of *Ptk7* during embryonic development

In mouse embryos, at E6.5, *Ptk7* is expressed in the early primitive streak. At E7.5, *Ptk7* is broadly expressed throughout the embryo, with high levels in the primitive streak. At E8.25-E8.75, *Ptk7* is highly expressed in the anterior and posterior regions of the primitive streak which is consistent with a role for *Ptk7* in neural tube closure [35]. In *Xenopus*, *Xptk7* is expressed in the neuroectoderm from late gastrula through all neurulation stages [35].

In zebrafish, *Ptk7* expression is ubiquitous at the shield stage and is pronounced in axial, paraxial and tailbud regions during late-gastrula stages. In the post-gastrulation stage, *Ptk7* is expressed in the head, neural tube and somites, with the highest level of expression

observed in the tailbud which persists until 24 hpf. The expression pattern of zebrafish *ptk7* is similar to that observed in *Xenopus* and mouse [94].

1.4.3 PTK7 and NTDs

The role of *Ptk7* in embryonic development ranges from axon guidance in *Drosophila* to the regulation of gastrulation, neural tube closure, neural crest migration, cardiac morphogenesis and epidermal wound repair in vertebrates [95]. Here I will mainly focus on its role in neural tube closure. *Ptk7* was first identified as an NTD responsible gene in a gene trapping screen for transmembrane proteins important for neural development. Mutant mice that were homozygous for a truncating mutation in *Ptk7* suffered from craniorachischisis that resulted from failure of neural tube closure initiation site 1. Besides the defects in the neural tube, the orientation of stereocilia bundles in the organ of Corti was also disrupted in these mice. Craniorachischisis and stereocilia orientation defects were also observed in *Vangl2* and *mScrib1* mutants (*Lp* and *Crc*, respectively). A strong genetic interaction was detected between *Ptk7* and *Vangl2* (*Lp*) where the frequencies of NTDs in the form of spina bifida increased dramatically from less than 10% (*Lp/+*) or zero (*Ptk7/+*) to 94% in double heterozygotes. No genetic interaction was observed between *Crc* and *Ptk7*. However, the NTD phenotype in *Lp/+; Ptk7/+* double heterozygotes was not as severe as in *Lp/+; Crc/+* double heterozygotes. The disruption in sensory hair cells orientation was also not observed in the *Lp/+; Ptk7/+* double heterozygotes.

Chuzhoi is an ENU-induced mutant which exhibits craniorachischisis and bundle orientation disruption in the inner ear. Abnormal lung and heart development were also observed in *chuzhoi* mutants. Genetic mapping and subsequent cloning showed that the underlying mutation in *chuzhoi* is a nucleotide substitution in *Ptk7* that created a new splice acceptor site leading to a 3 amino acid insertion in the protein, thereby resulting in disruption of *Ptk7* protein expression in *chuzhoi* mutants. *Chuzhoi* was also shown to genetically interact with *Vangl2/Lp* and *Celsr1/Crsh* but not with *Scrib/Crc* [96].

In the frog model, reduced expression of *Xptk7* by MOs (morpholino oligomers) also causes NTDs. This phenotype could be rescued by co-injection of full-length *Xptk7* or a construct lacking the cytoplasmic domain, indicating an important role of the membrane anchored extracellular domain in neural tube formation [35].

1.4.4 PTK7 and the Wnt pathways

Recruitment of Dsh to the membrane is essential for the activation of both canonical and non-canonical Wnt pathways. The pseudokinase domain of Ptk7 is required for this recruitment. Loss of function of *Fz7* does not affect Ptk7-mediated Dsh localization in animal caps. Interestingly, while overexpression of *Fz7* leads to recruitment and phosphorylation of Dsh, overexpression of *Ptk7* can recruit co-overexpressed *Dsh* to the membrane but no phosphorylated band was observed [97]. Rack1 is required for Ptk7-mediated Dsh membrane recruitment and the pseudo kinase domain of Ptk7 is necessary for Rack 1 translocation to the membrane. Furthermore, expression of a fusion construct consisting of a pseudo kinase domain-deleted mutant and Rack1 recruits Dsh to the membrane successfully suggesting that the pseudo kinase domain functions by recruiting Rack1 which in turn recruits Dsh independent of Fz [98]. These results seem to be inconsistent with the study of Lu et al. (2004) that demonstrated this domain to be dispensable in rescuing the NTD phenotype induced by injection of MOs against *Xptk7* in the frog model. This inconsistency could be due to the use of different functional assays: overexpression in cell lines versus a MO-knockdown in the frog. Alternatively, Ptk7 is a highly versatile protein implicated in many biological processes and hence recruitment of Dsh by its pseudo-kinase domain could reflect a functional aspect that is independent of PCP signaling.

Ptk7 co-precipitates with canonical Wnt3a and Wnt8 but not Wnt5a or Wnt11, indicating a role in canonical Wnt signalling [99], but Ptk7 inhibits rather than activates canonical Wnt activity. In *Xenopus*, Ptk7 inhibited secondary axis formation induced by Wnt8 or Wnt3a. The inhibition was also shown by siamois reporter assay which is readout of canonical Wnt pathway. The inhibition by Ptk7 is suggested to be upstream of β -catenin and Dsh. The non-canonical pathway was shown to be activated by Ptk7 through ATF2-based

luciferase reporter assay which is readout of the PCP pathway. For both the inhibitor and activator roles of Ptk7 in Wnt signalling, membrane-anchored extracellular part was shown to have the same activity as the full length one while the extracellular part alone or membrane-anchored intracellular part lost this inhibition or activation effect, indicating a crucial regulatory role of the membrane anchored extracellular domain of Ptk7 in canonical and non-canonical Wnt signalling. Ptk7 was suggested to act as a “molecular switch” that activates the Wnt/PCP non canonical pathway while inhibiting at the same time the Wnt/ β -catenin canonical pathway [99]. One contradictory study showed that Ptk7 physically interacts with β -catenin in a yeast two hybrid system and can activate the canonical Wnt pathway stimulated by Wnt3a. In the same study, they also showed that Ptk7 functions upstream of the β -catenin destruction complex in the Wnt canonical signalling pathway probably by stabilizing β -catenin [100].

A recent study confirmed the role of *ptk7* in zebrafish in both Wnt pathways and showed that this gene is also implicated in tailbud tissue differentiation. Overexpression of *ptk7* induces the expansion of dorsalization marker *chd* and the reduction of ventralization marker *vox* and β -catenin target *axin2*. Co-injection of zebrafish *ptk7* rescued the dorsoventral patterning defects induced by ectopic expression of *wnt8*. *ptk7* genetically interacts with *Wnt5b* in body length reduction caused by defective CE. Wnt11-induced cyclopia was also shown to be potentiated by *ptk7* overexpression [94]. In the same study, a mutant line made by a specifically engineered ZFN (zinc finger nuclease technology) showed that CE defects were observed in maternal-zygotic mutants, while this phenotype was absent in zygotic mutants demonstrating its important role in early embryo development [94]. Recently, another study by the same group described a skeletal defect observed in the zygotic mutant adult fish and demonstrated that this zebrafish model is an ideal model for idiopathic and congenital scoliosis [101]. One *PTK7* mutation found in a scoliosis patient was shown to disrupt both PCP and Wnt/ β -catenin signalling.

Lrp6 (Low-density lipoprotein receptor-related protein 6), a single-pass transmembrane protein, is required in Wnt/ β -catenin signalling and acts as a co-receptor for Wnt [102].

Dickkopf-1 (Dkk1), a secreted protein, negatively modulates the Wnt/ β -catenin pathway through its binding to Lrp6 [103]. The role of Dkk1 in modulating the canonical and non-canonical Wnt pathway was shown to be executed through the binding to Lrp6 or another membrane receptor Knypek (Kny) [104]. Lrp6 alone was also shown to be acting as a canonical and non-canonical Wnt pathway regulator with its different domains responsible for different functions [105]. Ptk7 was recently shown to modulate Wnt signalling activity via Lrp6 [64]. In HEK293 cells, PTK7 depletion by shRNA strongly inhibited LRP6 activation of β -catenin. Ptk7-depletion by MO caused a significant reduction of ectopically and endogenously expressed Lrp6 protein levels in *Xenopus*. Phenotypes of morphants of *Lrp6* and *Ptk7* are very similar. Lrp6 is also similar to Ptk7 in rescuing the neural tube closure phenotype caused by overexpressing *Wnt5* or *Wnt11*. Ptk7 was also shown to physically interact with different Lrp6 constructs as long as they have the transmembrane domain which leads to the hypothesis that Ptk7 modulates Wnt signalling activity by binding and stabilizing Lrp6.

Combining all the studies above, Ptk7 was shown to be very important modulator of both canonical and non-canonical Wnt pathways and represents a strong candidate gene for NTDs in humans.

1.4.5 PTK7 and other related genes

Cdx genes encode transcription factors controlling anterior-posterior patterning via integration of posteriorizing signals from retinoic acid and Wnt-canonical pathways [106]. They mediate neural tube closure through transcriptional regulation of *Ptk7* [107]. *Cdx1* and *Cdx2* double knock-out mice (DKO) showed the most severe NTD craniorachischisis. The observed defects in axis elongation and in somite morphology in these mutants were similar to the *Ptk7*-null mutant but not the *Vangl* or *Scribble* mutants. This is further supported by the fact that *Ptk7* expression was downregulated at E7.5 in *Cdx1/2* DKO mutants. In addition, ChIP (chromatin immunoprecipitation) analysis revealed that the 5' upstream promoter of *Ptk7* is responsive to the transcription factors Cdx1 and Cdx2. Combining all these data, Ptk7 is further implicated in the occurrence of NTDs.

Ptk7 was also demonstrated to be the primary cleavage target of the MT1-MMP (membrane type-matrix metalloproteinase) which cleaves ECM (extracellular matrix) proteins, initiates activation of soluble MMPs, and controls the functionality of cell adhesion and signalling receptors accompanied with other receptors including CD44. By reducing the expression of MT1-MMP in zebrafish using a MO, a body length reduction associated with PCP defects was observed and accumulation of full length Ptk7 in the 2-3 day old embryos was detected. A genetic interaction between *Ptk7* and *MT1-MMP* was shown by co-injections of low, sub-threshold dosages of *MT1-MMP* and *Ptk7* MO causing a synergistic effect on the CE phenotype [108].

In another cell migration and differentiation process which is called neural crest migration, Ptk7 precipitated with PlexinA at the gastrulation stage in *Xenopus*. Co-injection of *ptk7* aggravated the neural crest defects resulting from *Plexin A* injection alone [109]. Ptk7 was also shown to be needed for the facial branchiomotor (FBM) neuron migration. In E12.5 *Ptk7 chz* mutants, FBM neurons failed to migrate caudally [110].

Even though Ptk7 was implicated in the regulation of epithelial morphogenesis and PCP through modulation of the cytoskeleton, the underlying mechanism is not yet known. One possible pathway was raised and proven by the same group who first linked Ptk7 to NTDs [111]. The proto-oncogene tyrosine-protein kinase *Src* is traditionally considered to have an important role in cancer development. Endogenous *Src* and Ptk7 formed a complex in co-immunoprecipitation (coIP) experiments, and this interaction was dependent on the Ptk7 cytoplasmic domain. The glutathione S-transferase (GST) pull-down assay was further used to confirm this direct interaction. After testing this interaction with different domains of *Src*, Ptk7 was shown to directly interact with the SH3 domain of *Src*. The tyrosine kinase domain of Ptk7 is phosphorylated by active *Src* and then the interaction is fortified by direct interaction between this phosphorylated domain and the SH2 domain of *Src*. Reduced gene expression of *Ptk7* using short hairpin RNAs (shRNAs) in MDCK (Madin-Darby canine kidney) cells causes changes in cell shape from high and small apical surface to short and an

increased apical surface. The distribution of ROCK2 and the cytoskeletal proteins myosin IIB and actin was also affected in Ptk7-depleted MDCK cells compared to controls. Src-EGFP rescues all those phenotypes caused by *Ptk7* reduced expression. In conclusion, Ptk7 can regulate cell shape changes through Wnt signalling and/or interaction with Src in epithelial cells. Whether these two functional aspects of Ptk7 occur simultaneously or at different developmental stages or in different tissues remain unclear.

1.5 The Zebrafish Model for studies of convergent extension

1.5.1 Advantages of the zebrafish model

Zebrafish is recognized to be a good animal model to research developmental disorders mainly because of the following characteristics:

- a) It is evolutionally closer to humans than *Drosophila* and *C. elegans*.
- b) The genome of zebrafish was sequenced and is available publically at <http://zfin.org/>.
- b) It has a relatively short new generation producing period. It only takes 3-4 months for the larvae to mature to produce a new generation.
- c) More eggs from the same batch can be obtained compared with mice: around 200 eggs can be obtained from two fish every two weeks.
- d) During all of the early stages of development, the embryo growing outside of mother body is transparent which allows us to observe the phenotype without interfering with the normal progress.
- e) Availability of *in vitro* fertilization techniques and easier manipulation of microinjection compared to mouse.
- f) The cost of keeping the strain and producing new strains is relatively low.

1.5.1 Zebrafish development

Thanks to its inherent properties like *in vitro* fertilization and transparency of eggs, zebrafish development has been well studied and described in detail. Seven broad periods of development are defined: zygote, cleavage, blastula, gastrula, segmentation, pharyngula and hatching periods [112].

The zygote period is the period from fertilization to the formation of one cell at the animal pole. It occurs around 40 minutes post-fertilization in standard zebrafish incubation conditions. In this period, the chorion swells and lifts away from newly fertilized eggs and the non-yolky cytoplasm begins to stream toward the animal pole to form the first cell. In most cases, this is the best time for injection so that the injected content in yolk will diffuse to the cell.

The cleavage period is the period in which one cell will be divided six times via meroblastic cytoplasmic division. It occurs around until two hours post-fertilization. The blastomeres remain interconnected by cytoplasmic bridges before the fourth cleavage. From the fourth to the sixth cleavage, more and more blastomeres will have complete boundaries isolating them from others. In this period, eventual axes of body symmetry cannot be predicted from the orientation of the cleavage.

The blastula period is a period when the blastodisc begins to look like a ball. It lasts between 2.25 to 5.25 hours post-fertilization. Important processes occur during this blastula period: the embryo enters mid blastula transition (MBT), the yolk syncytial layer (YSL) forms, and epiboly begins.

The gastrula period is a period in which epiboly continues to finally cover all the yolk and finally the tail bud forms. It occurs between 5.25 to 10 hours post fertilization. During this period, a series of morphogenetic cell movements occur, producing the primary germ layers and the embryonic axis. CE movements of cells starting from shield stage play an important role in the epiboly and axis formation. Epiboly is a cell movement characterized as being a thinning and spreading of cell layers to finally engulf the whole yolk. According to the percentage of yolk coverage in lateral view, different epiboly stages are named. For example, 50% percent epiboly means the blastmere margin is in the middle between animal pole and vegetal pole.

The segmentation period is the period during which the somites develop, the primary organs start to become visible and the first body movements appear. It occurs around 24 hours post fertilization.

The pharyngula period is a period during which the pharyngeal arches develop rapidly. It occurs around 2 days post-fertilization. The embryos are morphologically distinct from other vertebrates.

The hatching period refers to the period when the embryo will escape from the chorion. It occurs around the end of the 3rd day of post-fertilization. During this period, rudiments of the pectoral fins, the jaws, and the gills develop rapidly.

1.5.2 CE in zebrafish

Neural tube formation in zebrafish implicates primary neurulation in the head and trunk and secondary neurulation in the tail as mentioned above in section 1.2.4. CE, as one of the very important processes for gastrulation and neurulation in zebrafish, happens after 50% epiboly when the cells surrounding the yolk migrate from ventral and lateral to dorsal regions. It consists of convergent and extension movements in different germ layers as demonstrated in **Fig. 9**. At the early blastula stage, cells located in the animal pole start to migrate to the vegetal pole. The cells at the blastoderm margin start to involute and form the prospective endoderm and mesoderm under the superficial layer of the prospective ectoderm. As endoderm and mesoderm originate from the same group of cells, the mechanisms involved in the separation of these two layers is not fully understood. These two layers will be discussed as combined in the following paragraphs.

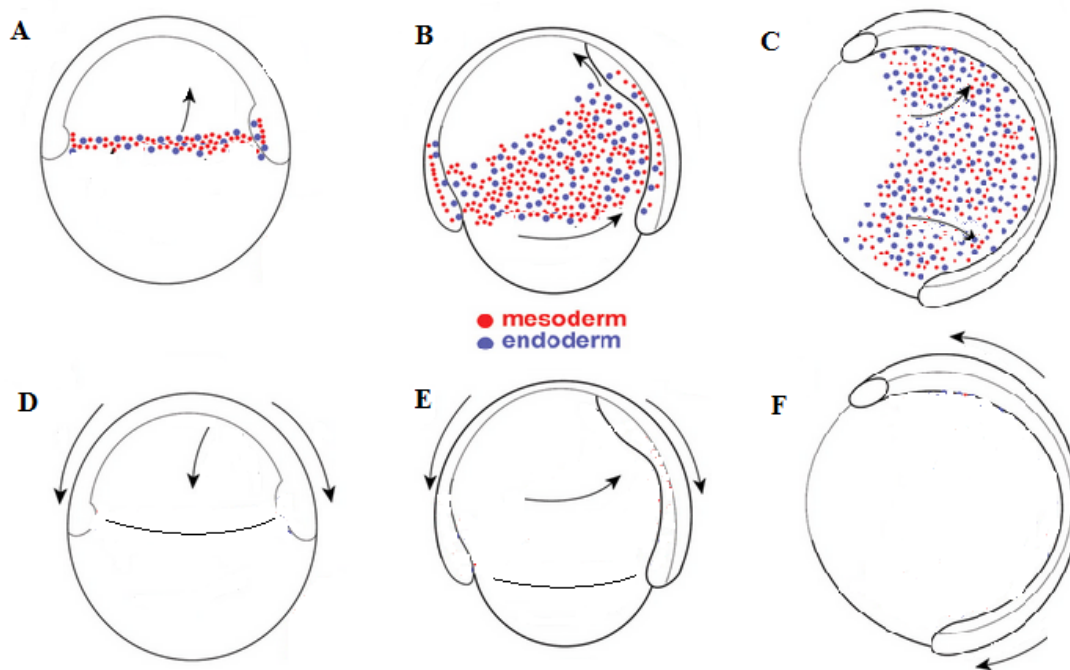


Fig. 9. Diagram for CE in zebrafish during gastrulation. At early gastrulation, mesendodermal cells form after involution from blastoderm margin cells and migrate mainly to the animal pole (A). Ectodermal cells basically migrate from the animal pole to the vegetal pole (D). At later stages, while migrating from the margin to the animal pole, ventro-lateral mesendodermal cells at the same time migrate to the dorsal midline (B). Overlying ectodermal cells continue the epiboly process and at the same time migrate from basal later to dorsal midline (E). At the end of gastrulation, mesendodermal cells continue migrating to the dorsal midline (C). Ectodermal cells elongate along the antero-posterior axis (F). All embryos were in lateral view with animal pole on the top and vegetal pole on the bottom. Modified from [113].

1.5.2.1 PCP genes and convergent extension in zebrafish

Mutations in *Wnt11* are responsible for the zebrafish mutant *slb* (silberblick) [114]. In zebrafish, *Wnt11* expression is first detected in the germ ring at the shield stage and later in the paraxial head mesoderm and in the neuroectoderm at 90% epiboly. The main phenotype of *slb*

mutant is cyclopia resulting from the abnormal extension of axial tissues. Even though it is not expressed in axial tissues, its expression in paraxial mesoderm is required for antero-posterior extension instead of medial-lateral convergence by affecting the mesoderm intercalation. Due to this extension defect of the axial mesoderm, the anterior end of the axial mesoderm cannot pass the edge of the ventral central nervous system which results in the fusion of the eyes (cyclopia). In these mutants, the body length is not significantly different from the wild type fish at later stages.

Ppt/*wnt5* (*pipetail*) is maternally provided, and zygotic expression of *Wnt5* is detectable in the germ ring at shield stage (remains at 50% epiboly, anterior-posterior and dorsal-ventral axes are detectable for the first time), and in the posterior paraxial mesendodermal cells at later gastrulation stage [115]. Due to the difference in their expression pattern, the *Wnt5* mutants mainly has CE defects in the posterior axial region while the defects in *Wnt11* mutant disperse along the whole antero-posterior axis. There is almost no effect on the extension at the anterior end of axis in *Wnt5* mutants which corresponds to the lack of cyclopia phenotype.

Knypek (*kny*) is a zebrafish mutant carrying mutations in the gene *glypican-4* which encodes for a heparan sulfate proteoglycan. It functionally interacts with *slb* in inducing the CE phenotypes like cyclopia [116]. This interaction was also seen with *trilobite* or *tri* (a homologue of *Vang* in zebrafish) [117]. It is important to note that although *kny*, *slb* and *tri* are mutants that all have the common convergent extension defects, the extent of these defects really differs among each other. The *kny* mutant shows the most severe reduction while the *slb* mutant shows only a slight reduction at 1dpf (day post-fertilization). For cyclopia, the *slb* mutant has the highest percentage while this phenotype is infrequent in *kny* mutants.

Trilobite is a zebrafish mutant of the PCP core gene *Stbm/Vang* that activates this pathway. The *tri* mutation in *Stbm/Vang* causes cell shape changes in the mesodermal and ectodermal cells and a reduction in the midline oriented migrating speed at the later gastrulation stage. This results in an obvious body length reduction at 1dpf. Cyclopia is also

observed in this mutant with a much lower frequency than in *slb* mutant. *Tri* also controls effective migration of branchiomotor neurons towards posterior rhombomeres [118]. Both reduced expression with MO against *tri* and ectopic overexpression of this gene can induce the same phenotype. Overexpression of *hVANGL1* in zebrafish gives the same CE phenotype [42].

Both gain- and loss-of function of another PCP gene *Pkl* cause CE defects [119]. Overexpression of a membrane-targeted intracellular domain of *Celsr* also causes a CE defect during zebrafish gastrulation [120].

1.5.2.2 Other genes mediating CE in zebrafish

Stat3 is a transcription factor responding to a variety of cytokines and growth factors. Zebrafish *Stat3* is activated by maternal Wnt/ β -catenin pathway in dorsal regions shortly after maternal blastula transition [121]. Reducing expression of this gene by MO shows CE defects like a short antero-posterior axis and mis-positioning of the head. Another study showed that *Stat3* affect the anterior movements of axial mesoderm and dorsal movements of non-axial mesoderm [122].

BMP signalling, FGF signalling and canonical Wnt signalling are all needed at some point in gastrulation to execute the CE process cooperatively [123].

1.5.2.3 PTK7 and CE in zebrafish

Knockdown of zebrafish *ptk7* by a zinc-finger nuclease (ZFN) gene targeting approach created a transgenic line with loss-of-function of *ptk7*. Heterozygous or homozygous mutants obtained from crossing of heterozygotes have no obvious phenotype while maternal-zygotic *MZPtk7* homozygous mutants show a very severe CE phenotype and body length reduction. Co-overexpression of *Ptk7* with *Wnt5b* showed that *Ptk7* exacerbates the CE phenotype caused by *Wnt5b* like cyclopia and body length reduction [94]. Interestingly, the CE phenotype observed in *MZptk7* mutants can be rescued by injection of the RNA products of membrane anchored extracellular *Ptk7* [94].

2 Research Project

2.1 Significance and rationale

NTDs are one of the most common congenital defects with a high incidence of 1-2 per 1000 births. They cause a heavy burden to both affected families and society. Although periconceptional folic acid supplementation has significantly reduced the frequency of NTDs by around 70%, roughly 30% of NTDs appear resistant to folic acid and these conditions still affect thousands of families each year. Epidemiological studies and data derived from animal models demonstrated a multifactorial etiology where environmental and genetic factors interact with each other to modulate their incidence and severity even though the underlying molecular and cellular pathological mechanisms remain poorly understood. Understanding the mechanisms underlying their etiology is a prerequisite to prevent their occurrence. The identification of NTD causing gene(s) would help investigate new aspects of the disease mechanisms and would certainly have a substantial impact on the best approach to choose for the development of new counseling and preventive strategies.

Genetic studies in animal models and human cohorts have demonstrated an important role for the PCP pathway in NTD pathogenesis. For some PCP members, such as *Vangl* and *Prickle*, their roles in human NTDs patients have been well documented [41, 45].

Ptk7 is a new PCP member in which mutations were shown to cause NTDs in two mouse lines [35, 96] and hence its orthologue represents a strong candidate for NTDs in humans. The role of *PTK7* in human NTDs has not been yet studied. As NTDs are etiologically complex, large human cohorts are needed to investigate the individual contribution of predisposing genes. Here, we recruited a large human NTD cohort and investigated the genetic contribution of *PTK7* to the occurrence of NTDs in this cohort.

2.2 Hypothesis and objectives

Hypothesis: Mutations in *PTK7* contribute to the pathogenesis of human NTDs.

Objective 1: Sequence analysis of the coding region of *PTK7* in a well characterized cohort of NTD patients and controls.

Objective 2: Genetic and bioinformatics validation of novel rare variants identified in *PTK7* in NTDs.

Objective 3: Functional validation of novel rare variants identified in *PTK7* in NTDs using a zebrafish model.

2.3 Material and Methods

2.3.1 Patients and controls

A cohort of 473 NTDs patients was recruited for this study. A total of 391 patients were recruited at the Spina Bifida Center of the Gaslini Hospital in Genova in collaboration with Dr. Valeria Capra and 82 patients were recruited at the Spina Bifida Center in Saint-Justine hospital in Montreal. Information on this cohort is included in Table 1.

Briefly, all patients (N=473) were affected with non-syndromic or isolated NTDs and were diagnosed according to Tortori-Donati classification [47]. The distribution of the major NTD forms in this cohort was as follows: 2% cranial, 46% open spinal and 52% closed spinal. Myelomeningocele was the major NTD present in this cohort at a frequency of 45%. The majority of NTD patients included in this cohort (97%) were white Caucasians. 19% of patients had a positive family history (Table 1).

The control group consisted of 639 ethnically-matched individuals including 433 Italian people and 206 Caucasians people of French-Canadian origin. Samples from patients

and controls were collected with the approval of the local ethics committees and written informed consent was obtained from all participating individuals.

Table 1. Characteristics of the 473 NTDs patients

Ethnic origin	459 Caucasian , 5 Hispanic, 3 Haitian, 4 North-African, 2 Middle Eastern Asiatic
Male sex (%)	44
Mean age (yr)	2.6
Cranial dysraphisms	11
Anencephaly	1
Cephalocele	10
Open spinal dysraphisms	215
Myelomeningocele	214
Myelocele	1
Closed spinal dysraphisms	247
Lipomyelomeningocele	37
Lipomyeloschisis	34
Terminal myelocystocele	1
Meningocele	12
Lipoma	48
Tight filum terminale	17
Dermal sinus	3
Diastematomyelia	17
Caudal Regression Syndrome	61
Unknown type	17

2.3.2 Re-sequencing of *PTK7*

The genomic structure of *PTK7* (ENSG00000112655) was determined using the NCBI (<http://www.ncbi.nlm.nih.gov>) and Ensembl (<http://www.ensembl.org>) public databases. Most recognized disease-causing mutations affect the protein-coding regions [124] and hence our screening strategy focused on the coding exons of *PTK7*. Primers flanking the exons and exon-intron junctions were developed to amplify the coding region and exon-intron junctions by PCR (polymerase chain reaction). Primers and corresponding exons are listed below in Table 2. Direct dye terminator sequencing of PCR products was carried out using the ABI Prism Big Dye Systems at the McGill University and Genome Quebec Innovation Center (Montréal, Québec, Canada). Samples were run on an ABI 3700 automated sequencer and analyzed using the SeqMan[®] sequence assembly and SNP discovery software (from DNASTAR[®]). Variants were confirmed by PCR and sequencing of the same patient.

2.3.3 Genetic validation of rare *PTK7* mutations

Rare mutations (minor allele frequency < 1%) identified in *PTK7* in NTD patients were genetically validated by: a) investigating their presence in the ethnically-matched controls and in the dbSNP (<http://www.ncbi.nlm.nih.gov/snp>), and The Exome Aggregation Consortium (ExAC) (<http://exac.broadinstitute.org/>) databases.; b) segregation in other family members when available and c) investigation of their *de novo* status when both parents were available.

2.3.4 Pathogenic effect prediction using bioinformatics

The possible effect of these mutations on the protein function was predicted by PolyPhen-2 (Polymorphism Phenotyping; <http://genetics.bwh.harvard.edu/pph2/dokuwiki/start>) and SIFT (Sorting Intolerant From Tolerant; <http://sift.jcvi.org/>). Polyphen predicts possible impact of an amino acid substitution on the structure and function of a human protein using straight-forward physical and comparative considerations. SIFT predicts whether an amino acid substitution affects protein function. SIFT prediction is based on the degree of

conservation of amino acid residues in sequence alignments derived from closely related sequences, collected through PSI-BLAST [125].

Table 2 Primers for sequencing of *hPTK7*

exons	forward_seq	reverse_seq	amplicon_size
1	GGACTCGGAGGTACTGGGC	GAGCCTCTCCACTACTCCAGG	387
2	ACACCTGCACTTACTGGACG	TGATAAATGCATTCTGCCTG	540
3	TTCCTTGTGTCTGTTGGCAC	TGAAGAGCACTGTGGTGGTG	356
4-5	CTTCCTCAGGCCGTTTCTC	AAAAGCAAAACATTCAACTGTGTC	702
6	TCAGCTTCCTTCTCTCTGCC	CCTACTCCCAGCATCCTTTTC	416
7	AGAGGATATGCAGAGGGCTG	ATTGGGAGCATAGTGGGACC	689
8-9	GGAAACTCCTGCCATCTGAG	TTTCAGCAGAGGGTGGGTAG	690
10	GAGCCAGCATGTCTTGGG	CTATACATCAGCCCTGCACTG	387
11-12	AGTTTGGACTTTGCCTGTGG	GATCACCAGGGAGCCATTC	668
13	ATCCTGGACCCACCAAG	CAGCAGCATGGTGAGACG	391
14	TGTTAAAGCCAGTGAAGGTGG	TCCAGGACCCAGCAACAG	461
15	GAGGCCCATGAAAGCAAAAATCC	ACGAAGGGCAGTGAATAACAGG	653
16	AGAACCGGGTCTCGTGC	GTAACAGCAGGCAGGTGAGG	497
17	TTTAAAGTTCTGCACTCCCAG	CAGTAACACATGTGAAGTTCTTACC	378
18	AGGAAGCTGAGGCTGTTGTG	CTATCCCAGGCCCTCCAG	422
19	CGCATGTGACCAATTTCTTG	GGTTGTATCTGTGTGCCTGC	447
20	CCAGCATTGCCCCAGAG	ACCTCAGCAATGCCTGTTG	411

2.3.5 Expression constructs

The human *PTK7*-pBluescriptR clone was obtained from Open Bio-systems (<http://dharmacon.gelifsciences.com/>) and used as a template to clone the full length ORF of

PTK7 in pCS2+ using the SLIC (sequence- and ligation-independent cloning) protocol [126]. Primers are depicted in Table 3. This master mix for PCR was as follows: 1.0 unit of PfuII polymerase, 1xGC buffer, 1.5 ul DMSO and 1X Betaine and 0.5 uM final concentration of forward and reverse primers in 50ul reaction volume. This PCR was conducted under the GC cycle: 98°C 1 minute, 98°C 10 seconds, 63°C 25 seconds, 70°C 2 minutes, 35 cycles. The pCS2+ vector was digested with BamHI and EcoRI. The PCR product and digested vector were purified using gel extraction kit (Bio Basic Inc) and then digested both with T4 polymerase in the absence of dNTP to produce the 5' overhangs that are homologous between the vector and inserts. The reaction was stopped by adding 1/10 volume of 10 mM dCTP. A ligation reaction was done using NEB ligase buffer in 37°C for 30 minutes. This is followed by transformation of the ligation product into XL-10 gold cells (Agilent Technology). Sequences of all constructs was verified by Sanger sequencing.

Human mutations were introduced in pCS2- *PTK7* using the protocol of site-directed mutagenesis. Primers used for mutagenesis are described in Table 3. All mutant constructs were verified by Sanger sequencing.

2.3.6. In vitro transcription

Capped mRNA for each of the pCS2+ expression constructs was obtained by *in-vitro* transcription using the mMESSAGEmMACHINE® SP6 Kit according to the supplied protocol (Ambion). DNA was linearized with the restriction enzyme NotI and precipitated by ethanol in the presence of NH₄ acetate. RNA synthesis was conducted with the presence of: 600 ng of linearized DNA, 2 ul Enzyme Mix, 1x NTP/CAP and 1x reaction buffer at 37°C for 2.5 hours. LiCl precipitation was used to collect the RNA. RNA was dissolved in RNAase free water and titrated.

Table 3. Primers for cloning and mutagenesis

Clone name	Method	Forward Primer 5'-3'	Reverse Primer 5'-3'
<i>hPTK7</i> -pCS2+	SLIC	TTGTTCTTTTGCAGCCACCATG GGAGCTGCGCGGGGATC	TATAGTTCTAGAGGCTCGAGTCACGG CTTGCTGTCCACGG
<i>hPTK7</i> -I121M-pCS2+	Mutagenesis	CGCCTCCTTCAACATGAAATGG ATTGAGGCA	TGCCTCAATCCATTCATGTTGAAGG AGGCG
<i>hPTK7</i> -V2911-pCS2+	Mutagenesis	CTGCTGCTGACCCAGATCCGGC CACGCAATG	CATTGCGTGCCGGATCTGGGTCAGC AGCAG
<i>hPTK7</i> -P345L-pCS2+	Mutagenesis	GTGTGACCTGCCTTCTCCCAAG GGTCTGCC	GGCAGACCCTTGGGGAGAAGGCAGG TCACAC
<i>hPTK7</i> -G348S-pCS2+	Mutagenesis	TGCCTTCCCCCAAGAGTCTGCC AGAGCCCA	TGGGCTCTGGCAGACTCTTGGGGGG AAGGCA
<i>hPTK7</i> -G775S-pCS2+	Mutagenesis	ACCAGCTTGGGCTCCAGCCCCG CGGCCACCA	TGGTGGCCGCGGGGCTGGAGCCCAA GCTGGT

2.3.7 Zebrafish Maintenance, mRNA and morpholino injection

Longfin zebrafish (*Danio rerio*) were raised from a colony maintained according to established procedures in compliance with guidelines set out by the Canadian Council for Animal Care. For the overexpression experiments, 400 pg capped message RNA were injected in one-cell stage zebrafish embryo. At 48 hpf (hours post-fertilization), the fish injected with RNA were dechorionated and photographed. Body length was measured with ImageJ.

2.3.8 Statistical analyses

For the distribution of rare variants in NTDs patients compared to controls, Chi-Square test was used. For the functional validation in zebrafish, cluster analysis was done using the SSPS statistics software. In wild-type *hPTK7* and mutant injected embryos, two cluster centroids were identified with mean body length ratios of 0.928 (grade 1: mildly affected) and of 0.531 (grade 2: severely affected), respectively. Then k-means clustering with classification was used to classify all additional cases from other experimental groups based

on the original cluster centroids. A Chi-square test was used to analyze the difference in distribution of the clusters among the experimental groups.

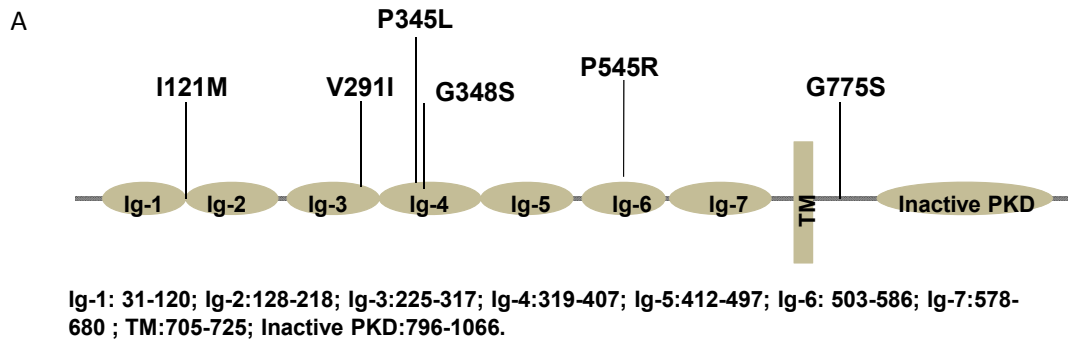
2.4 Results and Discussion

2.4.1 Results

We have identified 6 rare (MAF<1%) missense mutations in PTK7 in 6 NTD patients, two of which were novel and were absent in all 639 ethnically-matched controls and also absent from dbSNP and ExAC databases: p.Gly348Ser (c.1042G>A) and p.Gly775Ser (c.2323G>A). Three other rare missense mutations found in two NTDs patients were absent in ethnically matched controls but present in dbSNP and ExAC databases: p.Ile121Met (c.363C>G), p.Val291Ile (c.871G>A) and p.Pro345Leu (c.1034 C>T). One rare mutation, p.Pro545Arg (c.1634C>G) was present in one control while absent in all public databases (Table 4).

The potential pathogenic impact of all six rare missense variants identified in PTK7 in NTD patients was first evaluated in view of a) the degree of evolutionary conservation of the affected residue in the PTK7 protein family; b) the nature of the amino acid replacement and its possible impact on protein function; and c) possible co-segregation in additional family members (when available).

The variant p.Gly348Ser was identified in a 26-year-old Caucasian-Italian male diagnosed with lumbosacral myelomeningocele, Chiari II associated hydrocephalus. This mutation was transmitted by the mother and is shared also by one unaffected sister. It was absent from all controls analyzed and public databases. This variant is located in the extracellular Ig-like C type 4 domain (Fig. 10A). Glycine at position 348 is absolutely conserved among species analyzed (Fig. 10B). Replacement of a glycine with serine significantly reduces the hydrophobicity at this position and is considered a non-conservative change. This variant is predicted as probably damaging by Polyphen and tolerant by SIFT (Table 4).



B

	I121M	V291I	P345L G348S	P545R	G775S
human	↓ ASFNIKWIEA	↓ LLLTQVRPRN	↓ ↓ VTCLPPKGLPEPSVW	↓ DGSSLPEWVT	↓ SGPAATNKRH
chimpanzee	ASFNIKWIEA	LLLTQVRPRN	VTCLPPKGLPEPSVW	DGSSLPEWVT	SGPAATNKRH
dog	ASFNIKWIET	LLLTQVRPRN	VACLPPQGLPEPSVW	DGSSLPEWVT	SGPAATNKRH
cow	ASFNIKWLET	LQLTQVRPRN	VACPPQGLPEPSVW	DGSSLPEWVT	SGSAATSKRH
mouse	ASFNIKWIEA	LLLTQVRPRN	VTCPAPQGLPTPSVW	DGSSLPEWVT	SGPPATNKRH
chicken	ASFNIKWMET	LLITQVKARS	VSCACPRGVPTPQVW	DGSSLPSHVS	SSSGAS-KRH
zebrafish	TSFNIKWLES	LLITQVKQRN	VTCRAPYGHQPQEVW	DGSDMAVWVE	A--AGNKRH

Fig. 10. A) A schematic diagram showing the approximate distribution of the six rare variants identified in PTK7 in NTDs. B) Partial alignments of Ptk7 orthologues in humans, chimpanzee, dog, cow, mouse, chicken and zebrafish. The *PTK7* variants found in NTD patients affect conserved residues (indicated by arrows). Accession numbers: Human PTK7: NP_002812.2; Chimpanzee Ptk7:XP_518486.2; Dog Ptk7: XP_538929.2; Cow Ptk7: NP_001179894.1; Mouse Ptk7: NP_780377.1; Chicken Ptk7:NP_001026206.1; Zebrafish Ptk7: AGT63300.1

The variant p.Gly775Ser was detected in a 24-year-old Caucasian-Italian female diagnosed with caudal agenesis type II combined with absence of the coccyx and fibrolipoma of the filum. This mutation was absent from the patient's father, from controls and public databases. DNA from other family members was unavailable. As the only variant mapping to the intracellular part of the protein (Fig. 10A), glycine is highly conserved among species

analyzed except chicken where it is replaced by serine (Fig. 10B). Replacement of glycine with serine affects the hydrophobicity at this position. This variant was predicted by PolyPhen and SIFT to be benign and tolerant, respectively (Table 4).

The variant p.Ile121Met was detected in an 18-year-old male Caucasian-Italian patient diagnosed with myelomeningocele which is the most common form of open spina bifida. Detailed clinical information and DNA from family members were unfortunately not available for this patient. This variant was present in dbSNP (rs370537004 with undetermined MAF) and ExAC (allele frequency of 1.7×10^{-5}). This mutation is located immediately after the Ig like domain 1 of the protein (Fig. 10A) and affects a highly conserved isoleucine among all species (Fig. 10B). The hydrophobicity of Ile121 is not significantly affected by a methionine substitution; however, the latter does contain a sulphur atom that could affect the binding characteristics of the protein. This variant is predicted to be probably damaging by PolyPhen and intolerant by SIFT (Table 4).

The variant p.Val291Ile was identified in an 11-year-old Caucasian-Italian female diagnosed with lipomyelomeningocele which is a closed form of NTDs. The patient suffered from lipomyeloschisis associated to sacral schisis and hydromyelia from L3 to L5. The parents do not have any apparent form of NTDs. However, a paternal aunt of the proband was diagnosed with congenital scoliosis, and another maternal second-degree cousin was diagnosed with scoliosis and schisis at S1. This mutation was not present in the mother and the father DNA was not available and hence we could not determine if this mutation occurred *de novo*. The p.Val291Ile variant was detected in ExAC although with a very rare allele frequency of 1.6×10^{-5} . It is located in Ig like domain 3 (Fig. 10A) and affects a highly conserved valine residue among all species analyzed (Fig. 10B). Both valine and isoleucine are hydrophobic amino acids; however, a substitution with isoleucine introduces a bulky side chain, which may have structural or functional consequences. This mutation was predicted by PolyPhen and SIFT as probably damaging and intolerant, respectively (Table 4).

SNV ^a	Amino acid ^a	Freq. in patients (n=473)	Freq. in controls (n=639)	Freq. in dbSNP	Freq. in ExAC	Polyphen ^b	SIFT ^b
c.363C>G	p.Ile121Met	1 MMC	0	Unknown	1.6x10 ⁻⁵	+	+
c.817G>A	p.Val291Ile	1 LipoMMC	0	0	1.6x10 ⁻⁵	+	+
c.1034C>T	p.Pro345Leu	1 MMC	0	0.0012	7.8x10 ⁻⁴	-	-
c.1042G>A	p. Gly348Se	1 MMC	0	0	0	+	-
c.1634C>G	p.Pro545Arg	1 MMC	1	0	0	+	-
c.2323G>A	p.Gly775Ser	1 CA	0	0	0	-	-

^aThe SNV and amino acid numbering systems are based on *PTK7* cDNA and protein sequence with the accessions AF531868.1 and AAN04862.1 respectively.

^bPolyphen: +, probably or possibly damaging; -, benign; SIFT: +, not tolerated; -, tolerated. Abbreviations: CA, caudal agenesis; Freq., frequency; LipoMMC, lipomyelomeningocele; MMC, myelomeningocele; SNV, single nucleotide variant.

The variant p.Pro345Leu was identified in a 26-year-old Caucasian-Italian female diagnosed with lumbo-sacral myelocele associated to lipoma of the filum terminals and diastematomyelia. This mutation was not present in the mother but could not be tested in other family members. It was detected in dbSNP (rs143537049) and ExAc with an allele frequency of 0.0012 and 7.8 x 10⁻⁴ respectively. Pro345 is located in the Ig-like C type 4 extracellular domain (Fig. 10A). This residue is moderately conserved where it is only replaced by alanine in mouse and cysteine in chicken (Fig. 10B). The proline to leucine substitution is conservative and is predicted to be benign and tolerant by PolyPhen and SIFT, respectively (Table 4).

The variant p. Pro545Arg was detected in a myelomeningocele patient (we do not have the ethnic information). Additional clinical data for this patient as well DNA from other family members were unfortunately unavailable. This variant was present in one ethnically matched control while absent from public databases. The proline residue at position 545 maps to the Ig-like 6 extracellular domain and is highly conserved among all species except in zebrafish where it is replaced by alanine with similar amino acid characteristics (Fig. 10B).

The substitution of a nonpolar amino acid proline by a positively charged arginine is non-conservative. This variant is predicted to be possibly damaging and tolerant by PolyPhen and SIFT, respectively (Table 4).

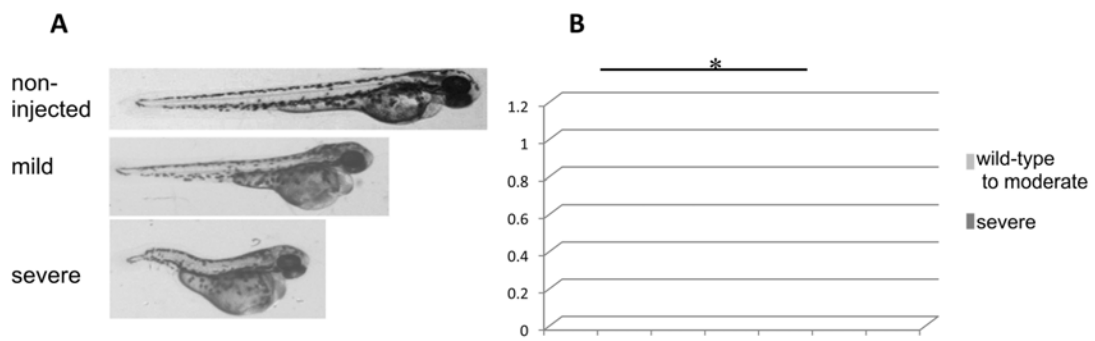


Fig. 11. A) Lateral views of 48 hpf zebrafish embryos showing the various degrees of severity of CE defects: uninjected or wild-type-like (top), moderately affected (middle) and severely affected (bottom). B) The distribution of the two clusters defined as grade 1(wild-type to moderate) or grade 2 (severe) with average body length ratios of 0.928 and of 0.531 respectively in each of the experimental groups injected with each of wild-type *PTK7* and of the 6 *PTK7* variants. Asterisk shows statistical significance at $P < 0.008$.

To further investigate the potential pathogenic role of rare *PTK7* variants identified in NTDs, we used an overexpression assay in a zebrafish model that represents a well established model for PCP-related studies [127]. Overexpression of PCP genes (including *VANGL1* and *PK1*) in zebrafish was shown to cause severe CE defects manifested mainly by a shortened body axis [42, 45]. Injection of 400 pg of wild-type or mutant *PTK7* produced a range of phenotypes that varied from wild-type to mild to severely affected embryos (Fig. 11A). Cluster analysis identified two centroids of average body length ratios of 0.928 (grade 1) and of 0.531 (grade 2). Overexpression of wild-type *PTK7* generated 63 % grade 1 and 37% of grade 2 embryos. Overexpression of each of the p.Ile121Met, p.Pro345Leu and Pro545Arg mutant RNAs generated less of the severely affected grade 2 embryos at $P=0.017$, $P=0.043$ and $P=0.029$, respectively (Fig. 11B). While this effect is not considered statistically significant after correction for multiple testing, these data suggest that these three alleles could

act in a hypomorphic fashion. Overexpression of the p.Gly348Ser RNA generated more of the severely affected grade 2 embryos, significant at $P=0.004$, suggesting a hypermorphic allele (Fig. 11B). Overexpression of either p.Val291Ile or p. Gly775Ser gave similar results as the wild-type PTK7 (Fig. 11B).

2.4.2 Discussion

Ptk7 was demonstrated to play an important role in regulating PCP signaling and loss-of-function of this locus is responsible for NTDs and other epithelial malformations in mouse models [35, 95]. In our study, we analyzed its human orthologue in a large cohort of various types of open and closed NTDs and we detected six rare variants in six NTD patients, three of which, p.Gly348Ser, Pro545Arg and Gly775Ser were novel. Four PTK7 variants detected in NTDs, p.Ile121Met, p.Val291Ile, p.Gly348Ser and p.Pro545Arg, were predicted to be pathogenic *in silico* by either Polyphen or SIFT or both. All variants except p.Gly775Ser, were located in the extracellular domain of PTK7 which was shown to be an important regulator of both non-canonical Wnt/PCP and canonical Wnt/ β -catenin signaling during embryonic development [94]. In fact, a membrane tethered extracellular domain of PTK7 was sufficient to rescue CE and patterning defects in maternal-zygotic (MZ) *ptk7* mutant zebrafish, demonstrating the importance of this domain in both pathways [94].

Functional validation using an overexpression assay in a zebrafish model demonstrated that three of the PTK7 rare mutations detected in NTDs, p.Ile121Met, p. Pro345Leu and p.Pro545Arg produced less severe CE defects suggesting that they could act as hypomorphs. This effect lost statistical significance after the stringent Bonferroni correction for multiple testing. It is interesting to note that another mutation at the same site as p.Pro545Arg, p.Pro545Ala, was identified in a single idiopathic scoliosis patient and his father (who did not display spinal deformities) and was shown to be a loss of function mutation that fails to rescue the PCP-mediated axial extension defects of *MZptk7* mutants and to inhibit the canonical Wnt/ β -catenin activity [101]. These data demonstrate that Pro545 is important for protein function and substitutions at this residue are most likely pathogenic. p.Pro545Arg was also present in one of control, The explanation could be that this heterozygous mutation alone is

not sufficient to cause spinal deformities, however combined with other genetic or environmental factors, spinal deformities could be induced. We also demonstrated that one variant, p.Gly348Ser, is most likely hypermorphic since it generated a higher percentage of severely affected embryos that was significantly different from wild-type.

PTK7 is a highly conserved protein with multiple functions during embryonic development and adult late-onset processes [95, 128]. In addition to its role in PCP signaling during gastrulation and neural tube closure, it is implicated in axonal guidance in *Drosophila* and in mediating neural crest migration and cardiac morphogenesis in vertebrates. In human pathological conditions, this versatile protein plays an important role in epidermal wound repair and its expression is frequently deregulated in cancer [95, 128]. A most recent study has demonstrated that embryonic loss-of-function in zebrafish leads to vertebral anomalies associated with congenital and idiopathic forms of scoliosis. In the same study, a novel sequence variant in *PTK7* with dysregulated Wnt signaling was identified in a single patient affected with idiopathic scoliosis, providing evidence for a pathogenic role for this gene in the human condition as well [101]. Remarkably, NTDs patients often show vertebral and spinal anomalies among them vertebral schisis, congenital scoliosis, cyphosis, lordosis, and shortened antero-posterior axis of the vertebral column. In particular an Italian patient carrying p.V291I mutation presents with a vertebral schisis and has a strong familial history of congenital scoliosis. (The p.V291I behaves *in vivo* as wild-type protein but it could be interesting evaluate the effect of this variant in late onset *ptk7* zebrafish mutants in spine morphogenesis, as done by Hayes et al. (2014). Our findings demonstrate for the first time a pathogenic role of this multifunctional gene in NTD etiology in humans. Moreover, since *PTK7* was demonstrated as an important later requirement in spine morphogenesis in animal models, we, in agreement with other, hypothesize that *PTK7* could also play a role in the correct patterning and development of the anteroposterior axis of embryo.

The molecular mechanisms by which *PTK7* can activate the non-canonical Wnt/PCP pathway and simultaneously inhibit the canonical Wnt/ β -catenin pathway remain largely undetermined. It was shown that the tyrosine kinase homology domain located in the

intracellular part of the protein is required for membrane recruitment of Dishevelled (Dsh), which is considered as a prerequisite for PCP signalling [97]. This recruitment seems to occur through the interaction of Ptk7 with Rack1 by its pseudokinase domain independent of Frizzled [98]. Interaction partners of the extracellular domain of Ptk7 have not yet been identified yet. Otk, the fly orthologue of Ptk7, interacts with Wnt4 and opposes canonical Wnt signalling in embryonic patterning. In *Xenopus* lysates, a deletion construct containing only the extracellular domain of Ptk7 was shown to selectively interact with Wnt3a and Wnt8, but not with Wnt5a and Wnt11 that are known inducers of non-canonical Wnt/PCP signaling. These data propose a model where Ptk7/Otk activates the non-canonical Wnt/PCP signaling by turning off the canonical signaling branch [99]. Five of the *PTK7* rare mutations identified in our NTD cohort in this study map to the extracellular domain and hence they could affect Wnt/PCP signaling indirectly through an over- or under-inhibition of the Wnt/ β -catenin canonical pathway. In particular, the variant p.Gly348Ser that behaved in a hypermorphic manner in the zebrafish assay would over-inhibit the canonical pathway leading to an over-activation of the PCP pathway and subsequent defective CE. Additional tests including luciferase gene reporter assays for both Wnt pathways are needed to further investigate this hypothesis and confirm the potential pathogenicity of these variants. Alternatively, these mutations could affect PCP signaling directly through yet to be determined *PTK7* binding partners or ligands.

2.4.3 Conclusions

In conclusion, we detected five rare missense mutations in *PTK7* with a potential pathogenic role, as predicted *in silico* and/or in the zebrafish overexpression assay, in 1.1% of the cohort analyzed. This is a very similar rate to the one reported in other screening studies of PCP genes in NTDs [129]. Our cohort analyzed in this study was also screened for mutations in other PCP genes and interestingly the patient who carried the p.Gly348Ser variant hypothesized to be hypermorphic carries a rare mutation in another PCP member CELSR1, p.Thr346Ser [130]. Note that this patient also has the published mutation FZD6*20C>T. Consistent with a multifactorial threshold model for NTDs, it would be interesting to test for genetic interactions among these two PCP variants detected in the same patient, for example

using a zebrafish model, to determine whether they act in combination to confer a higher risk for NTDs.

2.4.4 Future directions

2.4.4.1 Functional validation of PTK7 variants identified in NTDs

Co-injection experiments of wild type hPTK7 with all mutations separately will be conducted to determine whether the wild type and the mutants act in opposite directions to each other (dominant negative) or in the same direction in PCP signaling. In addition, *in vitro* experiments like the TCF/LEF reporter Luciferase assay in HEK293 cells transfected with wild type hPTK7 or the identified variants will be conducted to detect the effects of these mutations on canonical Wnt signaling. The ATF2-Based Luciferase reporter assay will be used to monitor the changes of non-canonical Wnt signaling [131]. For the mutations p.Gly348Ser, p.Pro345Leu, p.Pro545Arg, and p.Gly775Ser, their effect on the interaction with their potential partners such as β -catenin, RACK1 and LRP6 will be investigated by co-immunoprecipitation studies *in vitro* in HEK293 or in MDCK cell lines.

Knockdown/rescue experiments will be conducted in zebrafish using MO, an established technology that is the method of choice (preferred over RNAi) in zebrafish. To mimic completely the loss-of-function of a gene, a stable transgenic line will be produced by a new genome editing method CRISPR (clustered, regularly interspaced, short palindromic repeats)/Cas9(CRISPR associated system) [132].

2.4.4.2 Identification of more genes predisposing to NTDs

The complex etiology of NTDs involves the interaction of many genetic and environmental factors whose number and identity remain largely unknown. The use of innovative and powerful DNA sequencing methods to expand the genetic screen from one signaling pathway (PCP) to the entire coding genome by re-sequencing all the coding exons of affected individuals will increase the potential to systematically search and identify additional rare pathogenic mutations in both known and novel genes. Finally we are heading to a “whole

genome” sequencing era where new sequence technologies will allow whole genome mutation analysis including regulatory mutations without *a priori* assumption regarding genes function.

References

1. Copp, A.J., N.D. Greene, and J.N. Murdoch, *The genetic basis of mammalian neurulation*. Nature Reviews Genetics, 2003. **4**(10): p. 784-793.
2. Persad, V.L., et al., *Incidence of open neural tube defects in Nova Scotia after folic acid fortification*. Canadian Medical Association Journal, 2002. **167**(3): p. 241-245.
3. Melvin, E.C., et al., *Genetic studies in neural tube defects*. Pediatric neurosurgery, 2000. **32**(1): p. 1-9.
4. Kibar, Z., V. Capra, and P. Gros, *Toward understanding the genetic basis of neural tube defects*. Clinical genetics, 2007. **71**(4): p. 295-310.
5. Kinsman, S.L. and M.V. Johnston, *Congenital anomalies of the central nervous system*. Nelson Textbook of Pediatrics. 18th ed. Philadelphia, Pa: Saunders Elsevier, 2007: p. 2443-55.
6. James, W.H., *The sex ratio in anencephaly*. Journal of medical genetics, 1979. **16**(2): p. 129-133.
7. Van Allen, M.I., et al., *Evidence for multi - site closure of the neural tube in humans*. American journal of medical genetics, 1993. **47**(5): p. 723-743.
8. Mitchell, L.E., et al., *Spina bifida*. The Lancet, 2004. **364**(9448): p. 1885-1895.
9. Rodríguez, J.I. and J. Palacios, *Craniorachischisis totalis and sirenomelia*. American journal of medical genetics, 1992. **43**(4): p. 732-736.
10. Li, Z., et al., [*Prevalence of major external birth defects in high and low risk areas in China, 2003*]. Zhonghua liu xing bing xue za zhi= Zhonghua liuxingbingxue zazhi, 2005. **26**(4): p. 252-257.
11. Frey, L. and W.A. Hauser, *Epidemiology of neural tube defects*. Epilepsia, 2003. **44**(s3): p. 4-13.
12. Elwood, J.M., J. Little, and J.H. Elwood, *Epidemiology and control of neural tube defects*1992: Oxford University Press New York.
13. Shane, B. and E.R. Stokstad, *Vitamin B12-folate interrelationships*. Annual review of nutrition, 1985. **5**(1): p. 115-141.
14. Lumley, J., et al., *Periconceptional supplementation with folate and/or multivitamins for preventing neural tube defects (Review)*. Cochrane Database of Systematic Reviews, 2002(2).
15. Czeizel, A.E. and I. Dudas, *Prevention of the first occurrence of neural-tube defects by periconceptional vitamin supplementation*. New England Journal of Medicine, 1992. **327**(26): p. 1832-1835.
16. Wald, N., et al., *Prevention of neural tube defects: results of the Medical Research Council Vitamin Study*. International Journal of Gynecology & Obstetrics, 1992. **38**(2): p. 151.
17. Berry, R.J., et al., *Prevention of neural-tube defects with folic acid in China*. New England Journal of Medicine, 1999. **341**(20): p. 1485-1490.
18. De Wals, P., et al., *Spina bifida before and after folic acid fortification in Canada*. Birth Defects Research Part A: Clinical and Molecular Teratology, 2008. **82**(9): p. 622-626.

19. Hibbard, E. and R. Smithells, *Folic acid metabolism and human embryopathy*. The Lancet, 1965. **285**(7398): p. 1254.
20. Kirke, P., et al., *Maternal plasma folate and vitamin B12 are independent risk factors for neural tube defects*. Qjm, 1993. **86**(11): p. 703-708.
21. Daly, L.E., et al., *Folate levels and neural tube defects: implications for prevention*. Jama, 1995. **274**(21): p. 1698-1702.
22. Steegers-Theunissen, R., et al., *Neural-tube defects and derangement of homocysteine metabolism*. N Engl J Med, 1991. **324**(3): p. 199-200.
23. Steegers-Theunissen, R.P., et al., *Neural tube defects and elevated homocysteine levels in amniotic fluid*. American journal of obstetrics and gynecology, 1995. **172**(5): p. 1436-1441.
24. Mills, J.L., et al., *Homocysteine metabolism in pregnancies complicated by neural-tube defects*. The Lancet, 1995. **345**(8943): p. 149-151.
25. Frosst, P., et al., *A candidate genetic risk factor for vascular disease: a common mutation in methylenetetrahydrofolate reductase*. 1995.
26. Yamada, K., et al., *Effects of common polymorphisms on the properties of recombinant human methylenetetrahydrofolate reductase*. Proceedings of the National Academy of Sciences, 2001. **98**(26): p. 14853-14858.
27. Pejchal, R., et al., *Structural perturbations in the Ala → Val polymorphism of methylenetetrahydrofolate reductase: how binding of folates may protect against inactivation*. Biochemistry, 2006. **45**(15): p. 4808-4818.
28. McNulty, H., et al., *Riboflavin lowers homocysteine in individuals homozygous for the MTHFR 677C → T polymorphism*. Circulation, 2006. **113**(1): p. 74-80.
29. Molloy, A.M., et al., *The search for genetic polymorphisms in the homocysteine/folate pathway that contribute to the etiology of human neural tube defects*. Birth Defects Research Part A: Clinical and Molecular Teratology, 2009. **85**(4): p. 285-294.
30. Hall, J., M. Harris, and D. Juriloff, *Effect of multifactorial genetic liability to exencephaly on the teratogenic effect of valproic acid in mice*. Teratology, 1997. **55**(5): p. 306-313.
31. Chen, C.-P., *Chromosomal abnormalities associated with neural tube defects (II): partial aneuploidy*. Taiwanese Journal of Obstetrics and Gynecology, 2007. **46**(4): p. 336-351.
32. Harris, M.J. and D.M. Juriloff, *An update to the list of mouse mutants with neural tube closure defects and advances toward a complete genetic perspective of neural tube closure*. Birth Defects Research Part A: Clinical and Molecular Teratology, 2010. **88**(8): p. 653-669.
33. Harris, M.J. and D.M. Juriloff, *Mouse mutants with neural tube closure defects and their role in understanding human neural tube defects*. Birth Defects Research Part A: Clinical and Molecular Teratology, 2007. **79**(3): p. 187-210.
34. Kibar, Z., et al., *Ltap, a mammalian homolog of Drosophila Strabismus/Van Gogh, is altered in the mouse neural tube mutant Loop-tail*. Nature genetics, 2001. **28**(3): p. 251-255.
35. Lu, X., et al., *PTK7/CCK-4 is a novel regulator of planar cell polarity in vertebrates*. Nature, 2004. **430**(6995): p. 93-98.

36. Wang, Y., N. Guo, and J. Nathans, *The role of Frizzled3 and Frizzled6 in neural tube closure and in the planar polarity of inner-ear sensory hair cells*. The Journal of neuroscience, 2006. **26**(8): p. 2147-2156.
37. Curtin, J.A., et al., *Mutation of *Celsr1* Disrupts Planar Polarity of Inner Ear Hair Cells and Causes Severe Neural Tube Defects in the Mouse*. Current biology, 2003. **13**(13): p. 1129-1133.
38. Murdoch, J.N., et al., *Disruption of scribble (*Scrb1*) causes severe neural tube defects in the circletail mouse*. Human molecular genetics, 2003. **12**(2): p. 87-98.
39. Kinoshita, N., et al., *Apical accumulation of Rho in the neural plate is important for neural plate cell shape change and neural tube formation*. Molecular biology of the cell, 2008. **19**(5): p. 2289-2299.
40. Grumolato, L., et al., *Canonical and noncanonical Wnts use a common mechanism to activate completely unrelated coreceptors*. Genes & development, 2010. **24**(22): p. 2517-2530.
41. Kibar, Z., et al., *Mutations in VANGL1 associated with neural-tube defects*. New England Journal of Medicine, 2007. **356**(14): p. 1432-1437.
42. Reynolds, A., et al., *VANGL1 rare variants associated with neural tube defects affect convergent extension in zebrafish*. Mechanisms of development, 2010. **127**(7): p. 385-392.
43. Kibar, Z., et al., *Novel mutations in VANGL1 in neural tube defects*. Human mutation, 2009. **30**(7): p. E706-E715.
44. Kibar, Z., et al., *Contribution of VANGL2 mutations to isolated neural tube defects*. Clinical genetics, 2011. **80**(1): p. 76-82.
45. Bosoi, C.M., et al., *Identification and characterization of novel rare mutations in the planar cell polarity gene PRICKLE1 in human neural tube defects*. Human mutation, 2011. **32**(12): p. 1371-1375.
46. Purves, D. and J.W. Lichtman, *Principles of neural development* 1985: Sinauer Associates Sunderland, MA.
47. Rossi, A., et al., *Imaging in spine and spinal cord malformations*. European journal of radiology, 2004. **50**(2): p. 177-200.
48. Colas, J.F. and G.C. Schoenwolf, *Towards a cellular and molecular understanding of neurulation*. Developmental dynamics, 2001. **221**(2): p. 117-145.
49. Harland, R. and J. Gerhart, *Formation and function of Spemann's organizer*. Annual review of cell and developmental biology, 1997. **13**(1): p. 611-667.
50. Schoenwolf, G.C., *Microsurgical analyses of avian neurulation: separation of medial and lateral tissues*. Journal of Comparative Neurology, 1988. **276**(4): p. 498-507.
51. Burnside, B., *Microtubules and microfilaments in amphibian neurulation*. American Zoologist, 1973. **13**(4): p. 989-1006.
52. Schoenwolf, G.C. and M.V. Franks, *Quantitative analyses of changes in cell shapes during bending of the avian neural plate*. Developmental biology, 1984. **105**(2): p. 257-272.
53. Morita, H., et al., *Cell movements of the deep layer of non-neural ectoderm underlie complete neural tube closure in Xenopus*. Development, 2012. **139**(8): p. 1417-1426.
54. Karfunkel, P., *The mechanisms of neural tube formation*. International review of cytology, 1974. **38**: p. 245-271.

55. Karfunkel, P., *The role of microtubules and microfilaments in neurulation in *Xenopus**. Developmental biology, 1971. **25**(1): p. 30-56.
56. Karfunkel, P., *The activity of microtubules and microfilaments in neurulation in the chick*. Journal of Experimental Zoology, 1972. **181**(3): p. 289-301.
57. Quintin, S., C. Gally, and M. Labouesse, *Epithelial morphogenesis in embryos: asymmetries, motors and brakes*. Trends in genetics, 2008. **24**(5): p. 221-230.
58. Rolo, A., P. Skoglund, and R. Keller, *Morphogenetic movements driving neural tube closure in *Xenopus* require myosin IIB*. Developmental biology, 2009. **327**(2): p. 327-338.
59. Burnside, B., *Microtubules and microfilaments in newt neurulation*. Developmental biology, 1971. **26**(3): p. 416-441.
60. Suzuki, M., H. Morita, and N. Ueno, *Molecular mechanisms of cell shape changes that contribute to vertebrate neural tube closure*. Development, growth & differentiation, 2012. **54**(3): p. 266-276.
61. Griffith, C.M., M. Wiley, and E.J. Sanders, *The vertebrate tail bud: three germ layers from one tissue*. Anatomy and embryology, 1992. **185**(2): p. 101-113.
62. Greene, N.D. and A.J. Copp, *Development of the vertebrate central nervous system: formation of the neural tube*. Prenatal diagnosis, 2009. **29**(4): p. 303-311.
63. Shimokita, E. and Y. Takahashi, *Secondary neurulation: Fate - mapping and gene manipulation of the neural tube in tail bud*. Development, growth & differentiation, 2011. **53**(3): p. 401-410.
64. Bin-Nun, N., et al., *PTK7 modulates Wnt signaling activity via LRP6*. Development, 2014. **141**(2): p. 410-421.
65. van Amerongen, R. and R. Nusse, *Towards an integrated view of Wnt signaling in development*. Development, 2009. **136**(19): p. 3205-3214.
66. van Amerongen, R. and A. Berns, *Knockout mouse models to study Wnt signal transduction*. Trends in genetics, 2006. **22**(12): p. 678-689.
67. Kimelman, D. and W. Xu, *β -Catenin destruction complex: insights and questions from a structural perspective*. Oncogene, 2006. **25**(57): p. 7482-7491.
68. Grigoryan, T., et al., *Deciphering the function of canonical Wnt signals in development and disease: conditional loss-and gain-of-function mutations of β -catenin in mice*. Genes & development, 2008. **22**(17): p. 2308-2341.
69. Zeng, L., et al., *The Mouse *Fused* Locus Encodes Axin, an Inhibitor of the Wnt Signaling Pathway That Regulates Embryonic Axis Formation*. Cell, 1997. **90**(1): p. 181-192.
70. Barolo, S., *Transgenic Wnt/TCF pathway reporters: all you need is Lef?* Oncogene, 2006. **25**(57): p. 7505-7511.
71. Schuijers, J., et al., *Wnt - induced transcriptional activation is exclusively mediated by TCF/LEF*. The EMBO journal, 2014. **33**(2): p. 146-156.
72. Fanto, M. and H. McNeill, *Planar polarity from flies to vertebrates*. Journal of cell science, 2004. **117**(4): p. 527-533.
73. Wang, Y. and J. Nathans, *Tissue/planar cell polarity in vertebrates: new insights and new questions*. Development, 2007. **134**(4): p. 647-658.
74. Strutt, D., *Frizzled signalling and cell polarisation in Drosophila and vertebrates*. Development, 2003. **130**(19): p. 4501-4513.

75. Jenny, A. and M. Mlodzik, *Planar cell polarity signaling: a common mechanism for cellular polarization*. The Mount Sinai journal of medicine, New York, 2006. **73**(5): p. 738-750.
76. Rao, T.P. and M. Kühl, *An updated overview on Wnt signaling pathways a prelude for more*. Circulation research, 2010. **106**(12): p. 1798-1806.
77. Gerrelli, D. and A.J. Copp, *Failure of neural tube closure in the *loop-tail* (*Lp*) mutant mouse: analysis of the embryonic mechanism*. Developmental brain research, 1997. **102**(2): p. 217-224.
78. Enuka, Y., et al., *Epithelial sodium channels (ENaC) are uniformly distributed on motile cilia in the oviduct and the respiratory airways*. Histochemistry and cell biology, 2012. **137**(3): p. 339-353.
79. Huangfu, D., et al., *Hedgehog signalling in the mouse requires intraflagellar transport proteins*. Nature, 2003. **426**(6962): p. 83-87.
80. Huangfu, D. and K.V. Anderson, *Cilia and Hedgehog responsiveness in the mouse*. Proceedings of the National Academy of Sciences of the United States of America, 2005. **102**(32): p. 11325-11330.
81. Liu, A., B. Wang, and L.A. Niswander, *Mouse intraflagellar transport proteins regulate both the activator and repressor functions of Gli transcription factors*. Development, 2005. **132**(13): p. 3103-3111.
82. Smith, U.M., et al., *The transmembrane protein meckelin (MKS3) is mutated in Meckel-Gruber syndrome and the wpk rat*. Nature genetics, 2006. **38**(2): p. 191-196.
83. Kytälä, M., et al., *MKSI, encoding a component of the flagellar apparatus basal body proteome, is mutated in Meckel syndrome*. Nature genetics, 2006. **38**(2): p. 155-157.
84. Wallingford, J.B., *Planar cell polarity, ciliogenesis and neural tube defects*. Human molecular genetics, 2006. **15**(suppl 2): p. R227-R234.
85. Otto, E.A., et al., *Mutations in INVS encoding inversin cause nephronophthisis type 2, linking renal cystic disease to the function of primary cilia and left-right axis determination*. Nature genetics, 2003. **34**(4): p. 413-420.
86. Park, T.J., S.L. Haigo, and J.B. Wallingford, *Ciliogenesis defects in embryos lacking inturned or fuzzy function are associated with failure of planar cell polarity and Hedgehog signaling*. Nature genetics, 2006. **38**(3): p. 303-311.
87. Boutin, C., et al., *A dual role for planar cell polarity genes in ciliated cells*. Proceedings of the National Academy of Sciences, 2014. **111**(30): p. E3129-E3138.
88. De, A., *Wnt/Ca²⁺ signaling pathway: a brief overview*. Acta biochimica et biophysica Sinica, 2011: p. gmr079.
89. Kühl, M., et al., *Ca²⁺/calmodulin-dependent protein kinase II is stimulated by Wnt and Frizzled homologs and promotes ventral cell fates in Xenopus*. Journal of Biological Chemistry, 2000. **275**(17): p. 12701-12711.
90. Chou, Y.-H. and M.J. Hayman, *Characterization of a member of the immunoglobulin gene superfamily that possibly represents an additional class of growth factor receptor*. Proceedings of the National Academy of Sciences, 1991. **88**(11): p. 4897-4901.
91. Park, S.-K., H.-S. Lee, and S.-T. Lee, *Characterization of the human full-length PTK7 cDNA encoding a receptor protein tyrosine kinase-like molecule closely related to chick KLG*. Journal of biochemistry, 1996. **119**(2): p. 235-239.

92. Jung, J.-W., et al., *Cloning and characterization of the full-length mouse *Ptk7* cDNA encoding a defective receptor protein tyrosine kinase*. *Gene*, 2004. **328**: p. 75-84.
93. Jung, J.-W., et al., *Organization of the human PTK7 gene encoding a receptor protein tyrosine kinase-like molecule and alternative splicing of its mRNA*. *Biochimica et Biophysica Acta (BBA)-Gene Structure and Expression*, 2002. **1579**(2): p. 153-163.
94. Hayes, M., et al., *Ptk7 promotes non-canonical Wnt/PCP-mediated morphogenesis and inhibits Wnt/ β -catenin-dependent cell fate decisions during vertebrate development*. *Development*, 2013. **140**(8): p. 1807-1818.
95. Peradziryi, H., N.S. Tolwinski, and A. Borchers, *The many roles of PTK7: a versatile regulator of cell-cell communication*. *Archives of biochemistry and biophysics*, 2012. **524**(1): p. 71-76.
96. Paudyal, A., et al., *The novel mouse mutant, chuzhoi, has disruption of Ptk7 protein and exhibits defects in neural tube, heart and lung development and abnormal planar cell polarity in the ear*. *BMC developmental biology*, 2010. **10**(1): p. 87.
97. Shnitsar, I. and A. Borchers, *PTK7 recruits dsh to regulate neural crest migration*. *Development*, 2008. **135**(24): p. 4015-4024.
98. Wehner, P., et al., *RACK1 is a novel interaction partner of PTK7 that is required for neural tube closure*. *Development*, 2011. **138**(7): p. 1321-1327.
99. Peradziryi, H., et al., *PTK7/Otk interacts with Wnts and inhibits canonical Wnt signalling*. *The EMBO journal*, 2011. **30**(18): p. 3729-3740.
100. Puppo, F., et al., *Protein tyrosine kinase 7 has a conserved role in Wnt/ β - catenin canonical signalling*. *EMBO reports*, 2011. **12**(1): p. 43-49.
101. Hayes, M., et al., *ptk7 mutant zebrafish models of congenital and idiopathic scoliosis implicate dysregulated Wnt signalling in disease*. *Nature communications*, 2014. **5**.
102. Tamai, K., et al., *LDL-receptor-related proteins in Wnt signal transduction*. *Nature*, 2000. **407**(6803): p. 530-535.
103. Mao, B., et al., *LDL-receptor-related protein 6 is a receptor for Dickkopf proteins*. *Nature*, 2001. **411**(6835): p. 321-325.
104. Caneparo, L., et al., *Dickkopf-1 regulates gastrulation movements by coordinated modulation of Wnt/ β catenin and Wnt/PCP activities, through interaction with the Dally-like homolog Knypek*. *Genes & development*, 2007. **21**(4): p. 465-480.
105. Tahinci, E., et al., *Lrp6 is required for convergent extension during Xenopus gastrulation*. *Development*, 2007. **134**(22): p. 4095-4106.
106. Lohnes, D., *The Cdx1 homeodomain protein: an integrator of posterior signaling in the mouse*. *Bioessays*, 2003. **25**(10): p. 971-980.
107. Savory, J.G., et al., *Cdx mediates neural tube closure through transcriptional regulation of the planar cell polarity gene Ptk7*. *Development*, 2011. **138**(7): p. 1361-1370.
108. Golubkov, V.S., et al., *The Wnt/Planar Cell Polarity Protein-tyrosine Kinase-7 (PTK7) Is a Highly Efficient Proteolytic Target of Membrane Type-1 Matrix Metalloproteinase IMPLICATIONS IN CANCER AND EMBRYOGENESIS*. *Journal of Biological Chemistry*, 2010. **285**(46): p. 35740-35749.
109. Wagner, G., et al., *PlexinA1 interacts with PTK7 and is required for neural crest migration*. *Biochemical and biophysical research communications*, 2010. **402**(2): p. 402-407.

110. Glasco, D.M., et al., *The mouse Wnt/PCP protein Vangl2 is necessary for migration of facial branchiomotor neurons, and functions independently of Dishevelled*. *Developmental biology*, 2012. **369**(2): p. 211-222.
111. Andreeva, A., et al., *PTK7-Src signaling at epithelial cell contacts mediates spatial organization of actomyosin and planar cell polarity*. *Developmental cell*, 2014. **29**(1): p. 20-33.
112. Kimmel, C.B., et al., *Stages of embryonic development of the zebrafish*. *Developmental dynamics*, 1995. **203**(3): p. 253-310.
113. Nair, S. and T.F. Schilling, *Chemokine signaling controls endodermal migration during zebrafish gastrulation*. *Science*, 2008. **322**(5898): p. 89-92.
114. Heisenberg, C.-P., et al., *Silberblick/Wnt11 mediates convergent extension movements during zebrafish gastrulation*. *Nature*, 2000. **405**(6782): p. 76-81.
115. Kilian, B., et al., *The role of Ppt/Wnt5 in regulating cell shape and movement during zebrafish gastrulation*. *Mechanisms of development*, 2003. **120**(4): p. 467-476.
116. Topczewski, J., et al., *The zebrafish glypican knypek controls cell polarity during gastrulation movements of convergent extension*. *Developmental cell*, 2001. **1**(2): p. 251-264.
117. Marlow, F., et al., *Functional Interactions of Genes Mediating Convergent Extension, *knypek* and *trilobite*, during the Partitioning of the Eye Primordium in Zebrafish*. *Developmental biology*, 1998. **203**(2): p. 382-399.
118. Jessen, J.R., et al., *Zebrafish trilobite identifies new roles for Strabismus in gastrulation and neuronal movements*. *Nature cell biology*, 2002. **4**(8): p. 610-615.
119. Veeman, M.T., et al., *Zebrafish prickles, a modulator of noncanonical Wnt/Fz signaling, regulates gastrulation movements*. *Current biology*, 2003. **13**(8): p. 680-685.
120. Carreira-Barbosa, F., et al., *Flamingo regulates epiboly and convergence/extension movements through cell cohesive and signalling functions during zebrafish gastrulation*. *Development*, 2009. **136**(3): p. 383-392.
121. Yamashita, S., et al., *Stat3 controls cell movements during zebrafish gastrulation*. *Developmental cell*, 2002. **2**(3): p. 363-375.
122. Sepich, D.S., et al., *Initiation of convergence and extension movements of lateral mesoderm during zebrafish gastrulation*. *Developmental dynamics*, 2005. **234**(2): p. 279-292.
123. Yin, C., B. Ciruna, and L. Solnica-Krezel, *Convergence and extension movements during vertebrate gastrulation*. *Current topics in developmental biology*, 2009. **89**: p. 163-192.
124. Stenson, P.D., et al., *The human gene mutation database: 2008 update*. *Genome Med*, 2009. **1**(1): p. 13.
125. Kumar, P., S. Henikoff, and P.C. Ng, *Predicting the effects of coding non-synonymous variants on protein function using the SIFT algorithm*. *Nature protocols*, 2009. **4**(7): p. 1073-1081.
126. Li, M.Z. and S.J. Elledge, *Harnessing homologous recombination in vitro to generate recombinant DNA via SLIC*. *Nature methods*, 2007. **4**(3): p. 251-256.
127. Roszko, I., A. Sawada, and L. Solnica-Krezel. *Regulation of convergence and extension movements during vertebrate gastrulation by the Wnt/PCP pathway*. in *Seminars in cell & developmental biology*. 2009. Elsevier.

128. Lhoumeau, A.-C., et al., *PTK7: a cell polarity receptor with multiple facets*. Cell Cycle, 2011. **10**(8): p. 1233-1236.
129. De Marco, P., et al., *Planar cell polarity gene mutations contribute to the etiology of human neural tube defects in our population*. Birth Defects Research Part A: Clinical and Molecular Teratology, 2014. **100**(8): p. 633-641.
130. Allache, R., et al., *Role of the planar cell polarity gene CELSR1 in neural tube defects and caudal agenesis*. Birth Defects Research Part A: Clinical and Molecular Teratology, 2012. **94**(3): p. 176-181.
131. Ohkawara, B. and C. Niehrs, *An ATF2 - based luciferase reporter to monitor non - canonical Wnt signaling in xenopus embryos*. Developmental dynamics, 2011. **240**(1): p. 188-194.
132. Hwang, W.Y., et al., *Efficient genome editing in zebrafish using a CRISPR-Cas system*. Nature biotechnology, 2013. **31**(3): p. 227-229.